DEVELOPMENT OF SYSTEM SIMULATION TOOLS OF CENTRAL SOLAR HEATING PLANTS WITH A SEASONAL DUCT STORE IN THE GROUND

D. Pahud

April 1995

(updated in 1996)

With the collaboration of G. Hellström

Department of Mathematical Physics
Lund University
P. O. Box 118
S-221 00 Lund, Sweden

TABLE OF CONTENTS

ACKNOWLEDGEMENTS

The author would like to thank the following people for their help and advice throughout this study:

- Mr Göran Hellström, Department of Mathematical Physics at Lund University;
- Mr Jan-Olof Dalenbäck, Department of Building Service Engineering at Chalmers University of Technology in Göteborg;
- Mr Jean-Christophe Hadorn in Switzerland;
- Mr Kurt Källblad, Department of Building Science at Lund University.

Thanks also to Mrs L. Evans for her linguistic aid.

The author would also like to thank the *Swiss National Funds for Scientific Research* and the *Swedish Council for Building Research* (BFR) without whose aid this study would not have been possible.

1. INTRODUCTION

Large use of solar energy for heating purposes requires large heat storage facilities to overcome the seasonal discrepancy between the summer heat supply and the winter heat demand. Different types of heat stores in the ground have been extensively studied both from the practical and theoretical point of view. Included are water-based heat stores, e.g. pits and rock caverns, and duct ground heat stores, e.g. vertical coils in clay and boreholes in rock. Practical experience is more extensive for water stores than for ground stores.

However, duct ground stores are a very interesting alternative. Large stores can be achieved at a low cost, without requiring exclusive use of large ground surface area. Such stores have to be studied and optimised in a complete energy system. Duct ground heat stores fed by solar collectors are characterised by intensive heat transfer rates that last only part of a day. This phenomenon results in large temperature differences between the heat carrier fluid and the average temperature level of the store, and produces unnecessary quality losses. The use of a water buffer tank between the solar collectors and the store will improve the system's performance. In consequence, different possibilities of system operation are possible.

Research work is required to characterise such systems, in order to establish an optimal ratio between the different subsystems' size as well as to develop a strategy for an optimal system operation. Detailed and accurate system simulation programmes are required to perform such analysis.

This study has been carried out in the Department of Mathematical Physics at Lund University (Sweden), financed by a grant from the National Swiss Funds for Scientific Research, which was awarded by the Research Commission of the University of Geneva (Switzerland).

2. OBJECTIVES

The main objectives are to develop and produce reliable and accurate simulation tools of central solar heating plants with a seasonal duct store in the ground. These tasks involve:

- the set up of two systems' designs, comprising the complete system layout and connections between the different subsystems (system with and without short-term buffer tank);

- the build up of the simulation tools using a well known modular programme and existing modules (TRNSYS);

- the study of some aspects in order to check the validity of the existing modules in particular cases; find the limitations of the simulation tools;

- improvement of the existing modules when required (e.g. the duct store module);

- having reasonably fast simulation tools for practical use (according to the system layout);

- verification with more detailed programmes; (which tend to be time consuming and not as flexible).

The following topics are included in the present study:

- the effect of the weather data time-step on the thermal performances of a solar plant using a seasonal duct store in the ground;

- the effect when heat capacity is taken into account in the collector array or in the ground heat exchanger. The main features that a duct store model should present in order to compute the local process satisfactorily (temperature- and flow- dependent borehole thermal resistance, etc.);

- the build up of TRNSYS decks and verification with detailed programmes;

- the problem of passive solar gains. How they can be included in a simple load model. How they affect the load profile for a central solar plant during the heating period.

3. THE INFLUENCE OF THE WEATHER DATA TIME-STEP ON THE SIMULATED PERFORMANCES OF A SOLAR ENERGY SYSTEM WITH A SEASONAL DUCT HEAT STORE IN THE GROUND

3.1 Introduction

Unlike conventional heating technologies, the design of a central solar heating plant with seasonal storage (CSHPSS) is based on heat output (kWh) rather than the heat demand (kW). It requires design procedures that take several factors into consideration [1]. The final design is generally established with the help of detailed computer simulations, and relies on the ability of the computer programme to reproduce the physical behaviour of the planned system. Most of these computer programmes use hourly weather data, as most of the available weather data are recorded on an hourly basis.

The considered CSHPSS-system is composed of three main subsystems: an array of solar collectors, a seasonal duct store in rock and a distribution network delivering the heat to the consumer (heat load). No heat pump is used in the system; it is designed to be operated at medium or high temperature. The collector array is directly coupled to the duct store in rock via a heat exchanger. Duct stores in soil (clay, dry moraine, etc.) are governed by the same thermal processes [2]. An example of flat plate collectors coupled to a duct store in moraine has been realised in Geneva (Switzerland) and carefully measured [3, 4].

In a system using a duct store, the heat rate exchanged with the store is mainly determined by the difference between the temperature level of the heat carrier fluid and the ground in the immediate vicinity of the borehole. The precision of the calculation will depend on the ability to reproduce the rapid temperature variation of the heat carrier fluid heated by the solar panels. The time-step at which weather data is provided will also have an effect on the temperature variations and thus the calculated performances.

The objective of this chapter is to assess the influence of the weather data time-step on the overall performances of a typical solar heating system using a seasonal duct store. This study is primarily aimed at testing the validity of the duct store model. Another study concerning the interaction between a solar collector field with heat capacity and a duct store has been carried out and presented in the next chapter. A reference system is defined and used to perform a case-study.

3.2 Methodology

The system design will be described in section 3.4. A reference system is defined by a typical set of parameter values that characterise the solar collectors, heat store, heat exchangers, flow rates and the heat load. The overall performances of the system are then calculated using high resolution weather data, containing the outdoor temperature and the global incident radiation on a two-minute basis.

The effect of the weather data time-step is expected to be greater when the interactions between the collector array and the duct store are the strongest. They occur when the incident solar radiation varies quickly with large amplitudes. The intention is to estimate the maximum magnitude of the effect on the overall performance of the system. Simulations are restricted to a typical summer month of weather data (June), which is characterised by a large amount of incident energy and fast variations of the incident radiation. The influence of the weather data time-step is assessed under the following conditions:

- The weather data has been measured at Nykvarn in Sweden; (northern location; latitude: 59.2°; longitude: 17.4° East). The global incident radiation was measured in a plane facing south and tilted to 38°. It was recorded every two-minutes together with the outdoor temperature. The month of June 1988 was chosen for the simulations. The daily values of the incident insolation range from 0.5 to 8.1 kWh/m^{2}day, with a mean value of 5.2 kWh/m^{2}day. The measured incident radiation sometimes exceeds 1'200 W/m^2, and on some days exhibits large and rapid variations (see Fig. 3.1).
- The thermal performances of the solar collectors are calculated without heat capacitive effects. As a consequence, the variations of the collected heat rate, following those of the incident radiation, will not be damped down by the collector array. It will stress the dynamic behaviour of the interaction between the solar panels and the duct store.
- The interactions between the collector array and the duct store result in rapid temperature variations of the heat carrier fluid in the ground heat exchanger. These temperature variations occur during part of a day and will only propagate through a limited rock region around each borehole (less than 1 m radius). They are not affected by the heat losses of the store. A precise computation of the system's heat balance is not the objective here. The heat losses of the duct store are thus not calculated.

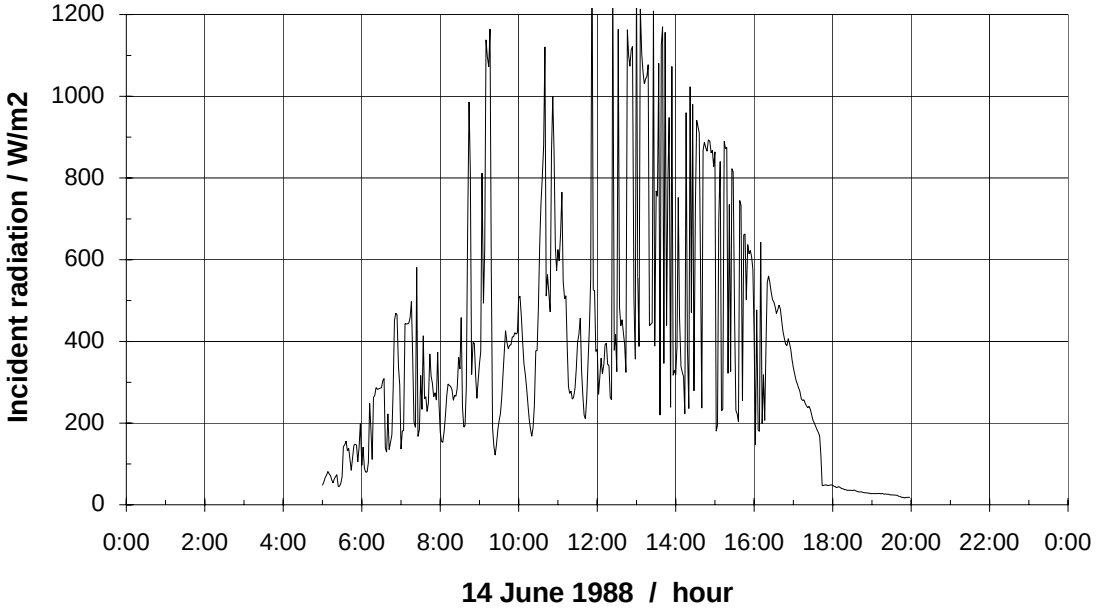

Fig. 3.1 Incident radiation measured every two-minutes the 14th June 1988 at Nykvarn (Sweden).

For each simulation, the following quantities are calculated:

- Total energy collected by the solar array.
- Net heat injected into the store.

- Total energy supplied by the boiler.
- Temperature average of the heat carrier fluid entering the store during injection.
- Temperature average of the heat carrier fluid leaving the store during extraction.
- Maximum temperature of the heat carrier fluid in the store.

Other weather data sets are generated based on the two-minute values. These latter values are averaged on different time scales, ranging from 10 minutes up to 24 hours, resulting in 144 different weather data sets. The influence of the weather data time-step is then assessed by comparing the calculated quantities from simulations with the different data set. The whole procedure is repeated with different sets of parameters in order to explore the sensitivity to different system parameters.

3.3 Duct Store Models

3.3.1 DST Model

The DST model [5] is a simulation model for ground heat storage systems. It simulates a stand-alone heat store with user specified loading conditions. The mutual influences with other components of an energy system are not included in the simulation. For this purpose, a version has been developed [6] for TRNSYS [7], a well-known modular programme for the simulation of partial or complete energy systems. The following description concerns the "stand alone" DST version.

The store volume has the shape of a cylinder with a vertical symmetry axis. The ducts are assumed to be uniformly placed within the store volume. There is convective heat transfer in the ducts and conductive heat transfer in the ground. The temperature in the ground is represented by three parts: a global temperature, a local solution and a steady-flux part. The global and the local problem are solved with the use of the explicit finite difference method (FDM), whereas the steady-flux part is given by an analytical solution. The total temperature at a point is obtained by a superposition of these three parts.

The short-time effects of the injection /extraction through the ducts are simulated with the local solutions, which depend only on a radial coordinate and cover the cylindrical volume ascribed to each duct (or borehole). The outer surface of the volume is totally insulated. The heat transfer from the fluid to the ground in the immediate vicinity of the duct (or borehole) is calculated with a constant heat transfer resistance. A steady-state heat balance for the heat carrier fluid gives the temperature variation along the flow path. (The heat capacitive effects of the fluid are not taken into account.) The local solution may account for a radial stratification of the store temperatures (due to series-connections of the ducts (or boreholes)), as well as a vertical division of the store volume.

The slow redistribution of heat during injection /extraction and the interaction between the store region and the surrounding ground are accounted for by the steady-flux and the global solution. The simulated ground volume is divided into a two-dimensional mesh using a radial and vertical coordinate. The model assumes homogeneous and constant thermal properties within the store volume. In the surrounding ground they may vary from node to node. Insulation may be put anywhere along the surfaces of the store volume, on the ground surface or in the surrounding ground. A time-varying temperature is given on the ground surface.

The main differences between the DST version for TRNSYS and the "stand alone" DST version are:

- A radial stratification of the store temperatures is not possible, as all the ducts (or boreholes) are assumed to be coupled in parallel.
- A vertical division of the store volume is not possible when computing the local solutions.

A more recent DST version for TRNSYS [8] has removed these differences and can account for a flow- and temperature-dependent borehole thermal resistance, as well as for the heat exchange between the ducts in the borehole.

3.3.2 Detailed Duct Store Models

Two models have been developed that are restricted to a detailed computation of the local solutions in a duct store. They differ only by the heat capacitive effects of the heat carrier fluid, taken into account in one and not in the other. The model without heat capacitive effects permits comparisons with the DST model. They consider one cell formed by the ground volume ascribed to one borehole. There is a convective heat flow along the borehole and a transverse heat exchange between the fluid and the ground. The heat transport in the ground is supposed to take place solely by conduction. It is computed by the finite difference method (FDM), in the two-dimensional axis-symmetrical geometry of the cell (radial and vertical mesh). The vertical heat conduction is neglected. The outer surface of the cell is perfectly insulated and the ground is represented by homogeneous and constant thermal properties.

The models assume open annular ducts coupled in parallel: a single pipe is inserted to the bottom of the borehole to inject or extract the fluid flowing in direct contact with the ground (between the borehole wall and the pipe). A convective heat flow along the flow path (in the pipe and the annular channel), is computed according to the vertical mesh. Combined with the conductive heat flow through the inner pipe and the borehole wall, a new temperature profile of the fluid is calculated at the end of every time-step. The heat transfer resistances are calculated according to the flow rate and temperature of the heat carrier fluid [2] (the inner pipe is assumed to be centred). If the heat capacitive effects of the fluid are not taken into account, the heat transfers are computed as in the DST model, but with a flow- and temperature- dependent borehole thermal resistance.

3.4 System Design and Simulation Programmes

The system design (see Fig. 3.2) is very simple and has proved its efficiency and reliability with systems using water store [9]. The design is very similar to that used extensively in the analysis of systems using duct store with the MINSUN programme [10, 11]. An important difference is that direct connection between the collector array and the distribution network is taken into consideration in the present study. No buffer store is used between the solar collectors and the duct store. This would make the temperature variations of the heat carrier fluid in the duct store smoother, which is not the intention in this study.

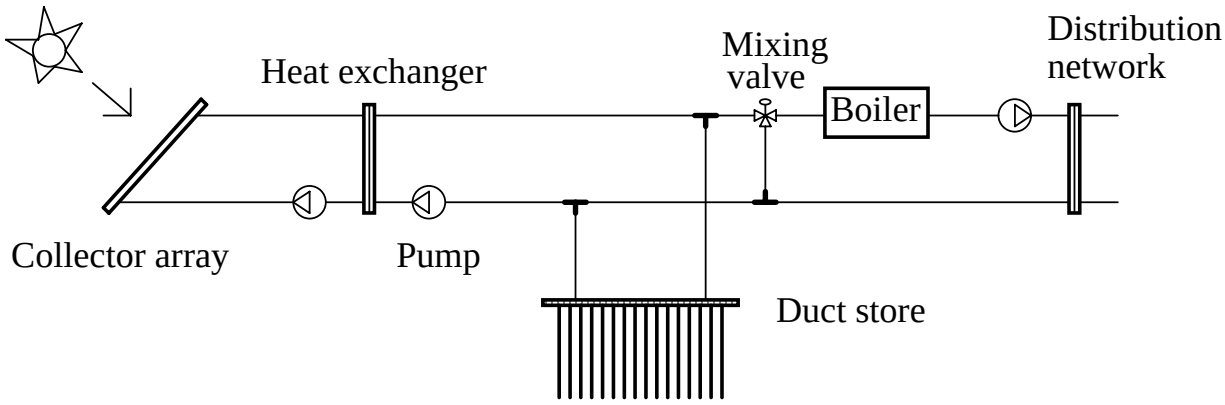

Fig. 3.2 Design of the simulated system.

The solar collectors are characterised by a linear efficiency. The flow rate is set to a constant value when usable solar gains are available. Their performances are calculated together with the solar heat exchanger, using the modified collector heat removal factor F_R' [12]. The flow rates have the same value on both sides of the heat exchanger; (they are called "loading flow rates"). The incidence angle modifier (IAM) is not considered in the calculations.

The ground heat exchanger of the duct store is formed by vertical boreholes arranged in a hexagonal pattern. Calculations assume a parallel coupling of the boreholes (see section 3.3.2).

The heat load is reduced to the domestic hot water requirements (heat losses included). A pre-defined daily profile is given hour by hour, which exhibits peak power demand early in the morning, at noon and in the evening (see Fig. 3.3). The forward temperature on the primary side is set to a typical value of 55 °C, using a boiler if necessary. The mixing valve ensures that the forward temperature does not exceed its prescribed value (55 °C). It also permits the disconnection of the solar collectors and the duct store from the rest of the system, if the forward temperature (before the boiler) is lower than the return temperature. The return temperature is assumed to be constant (30°C). A variable flow rate allows the heat requirement to be met.

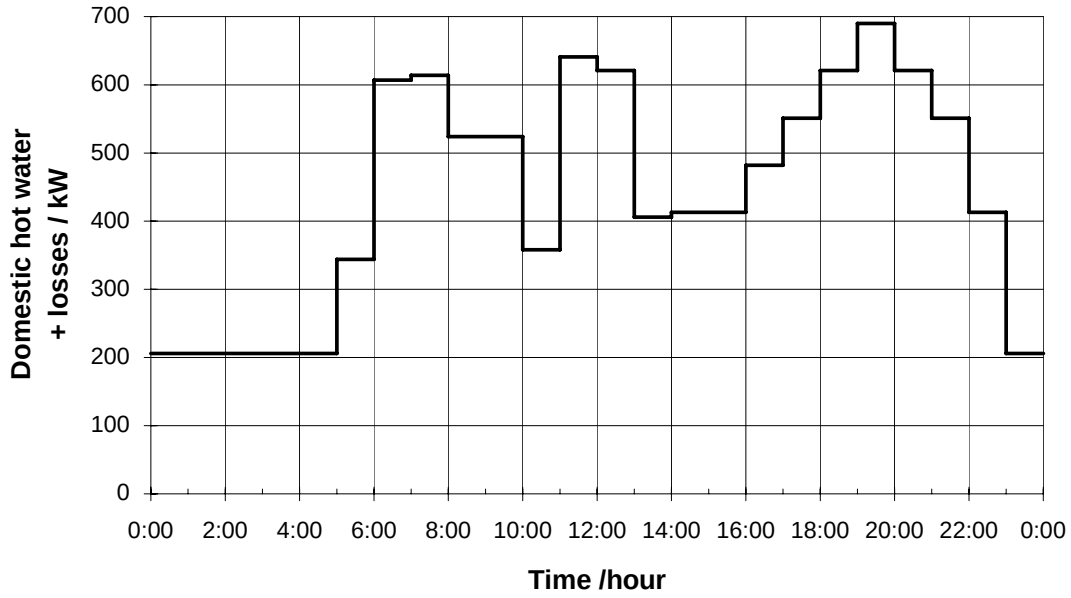

Fig. 3.3 Daily profile of the domestic hot water requirement (heat losses included).

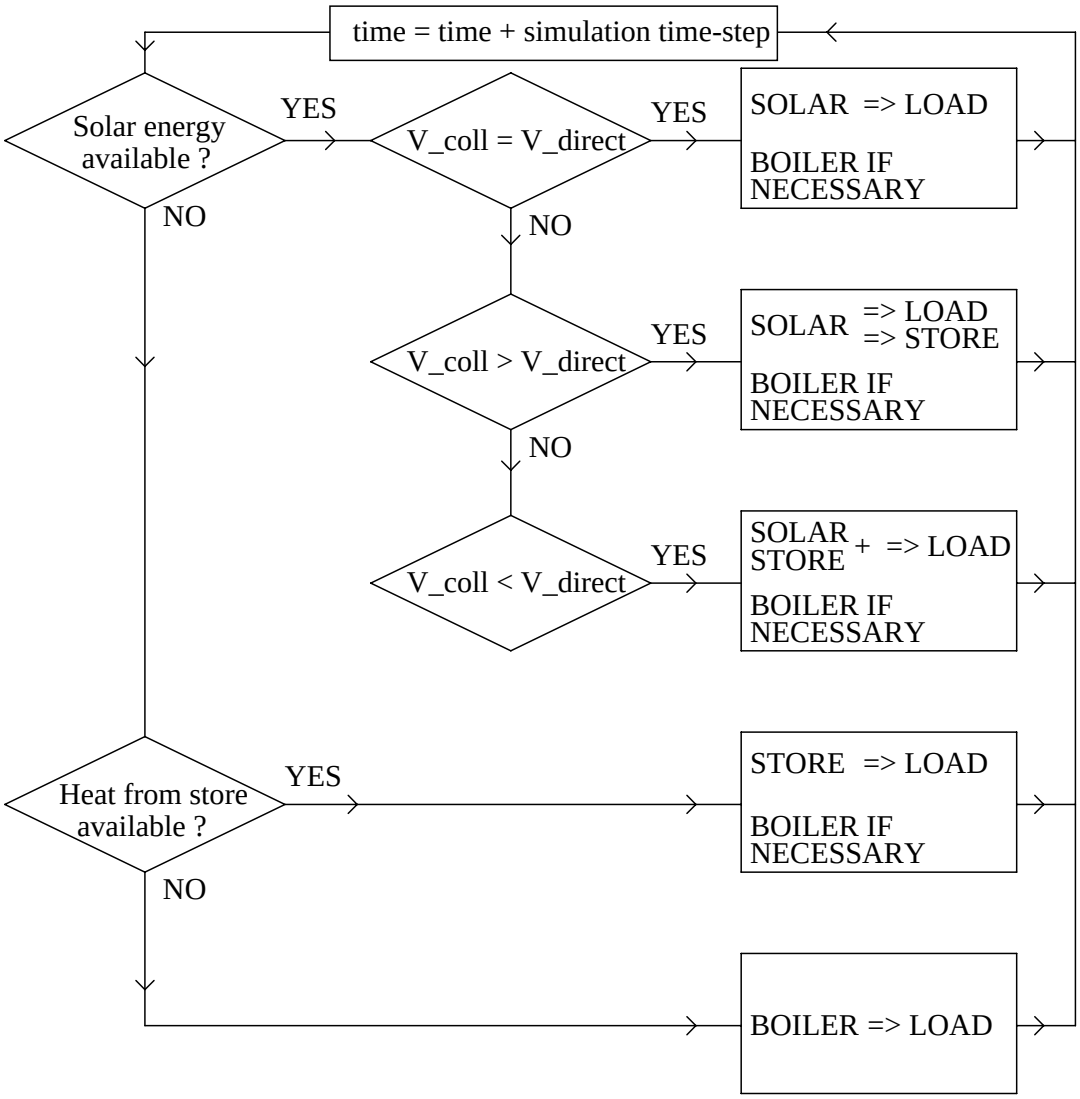

Fig. 3.4 Flow chart defining the operation strategy of the system. V_coll is the flow rate in the solar heat exchanger and V_direct is the flow rate which transits from the store and/or the solar heat exchanger to the boiler.

The detailed programmes (see section 3.3.2) calculates the heat flow and associated temperature levels throughout the system for every time-step, according to the flow chart given in Fig. 3.4. The system control gives priority to the collection of the solar gains, regardless of the electric energy consumed by the pumps. In consequence, solar gains are collected as soon as they are usable. This corresponds to a collector controller whose dead-band temperature differences are set to 0 K. The simulation time-step is very short (a few tenths of seconds), as a consequence of the computation of the detailed thermal process inside the boreholes. The parameters defining the reference system are reported in table 3.1. The size corresponds to an annual load of approximately 10'000 MWh. It should be noted that the system is not economically optimised to produce heat at the lowest cost.

Solar collectors:	
Location:	latitude: 59.2° North
	longitude: 17.4° East
Orientation:	azimuth: 0° (South facing)
	tilt angle (with respect to horizontal plane): 38°
Area:	35'000 m^2
Specific flow rate:	0.007 kg/sec /m^2 of collector area (loading flow rate)
Heat carrier fluid:	water
Average transmittance-absorptance product:	
	0.75 (-) (corrected by the collector efficiency factor F')
Overall loss coefficient:	3.5 W/m^2K (corrected by the collector efficiency factor F')
Solar heat exchanger (counter flow)	
UA_value:	120 W/K /m^2 of collector area
Specific flow rate secondary side:	
	0.007 kg/sec /m^2 of collector area (loading flow rate)
Duct heat storage	
Volume:	350'000 m^3
Depth:	125 m
Number of boreholes:	359
Ground heat exchanger:	
	heat carrier fluid: water
	open annular duct, hexagonal pattern
	spacing between boreholes: 3 m
	borehole diameter: 0.115 m
	inner pipe: outer diameter: 0.063 m
	thickness wall: 0.0058 m
	thermal conductivity of pipe material: 0.2 W/mK
Rock:	thermal conductivity: 3.5 W/mK
	volumetric heat capacity: 2.2 MJ/m^3K
Initial store temperature (1st June):	
	47 °C
Heat load	
Domestic hot water (including heat losses):	
	≈ 10 MWh/day
Forward temperature:	55 °C
Return temperature:	30 °C

Table 3.1 Parameters defining the reference system.

Extensive checks of the programme have been performed. Different versions were created to take into account the heat capacity of the collector array, or the effect of a buffer tank (see sections 3.6 and 3.7). A version without heat capacitive effects of the ground heat exchanger allowed a comparison of the results with a TRNSYS system using the DST component (see chapter 5). In this version, the thermal borehole resistance was set to a constant value and the vertical division of the store volume was reduced from 5 to 1 cell. In the TRNSYS system, the

DST component was totally insulated. The excellent correspondence between the two calculations made us confident with our own programmes.

3.5 Calculations and Results

3.5.1 Weather Data Time-step Effect

The effect of the weather data time-step is illustrated in Fig. 3.5. The thermal performances of the reference system are calculated for 145 different time averages of weather data, ranging from two-minute up to daily values.

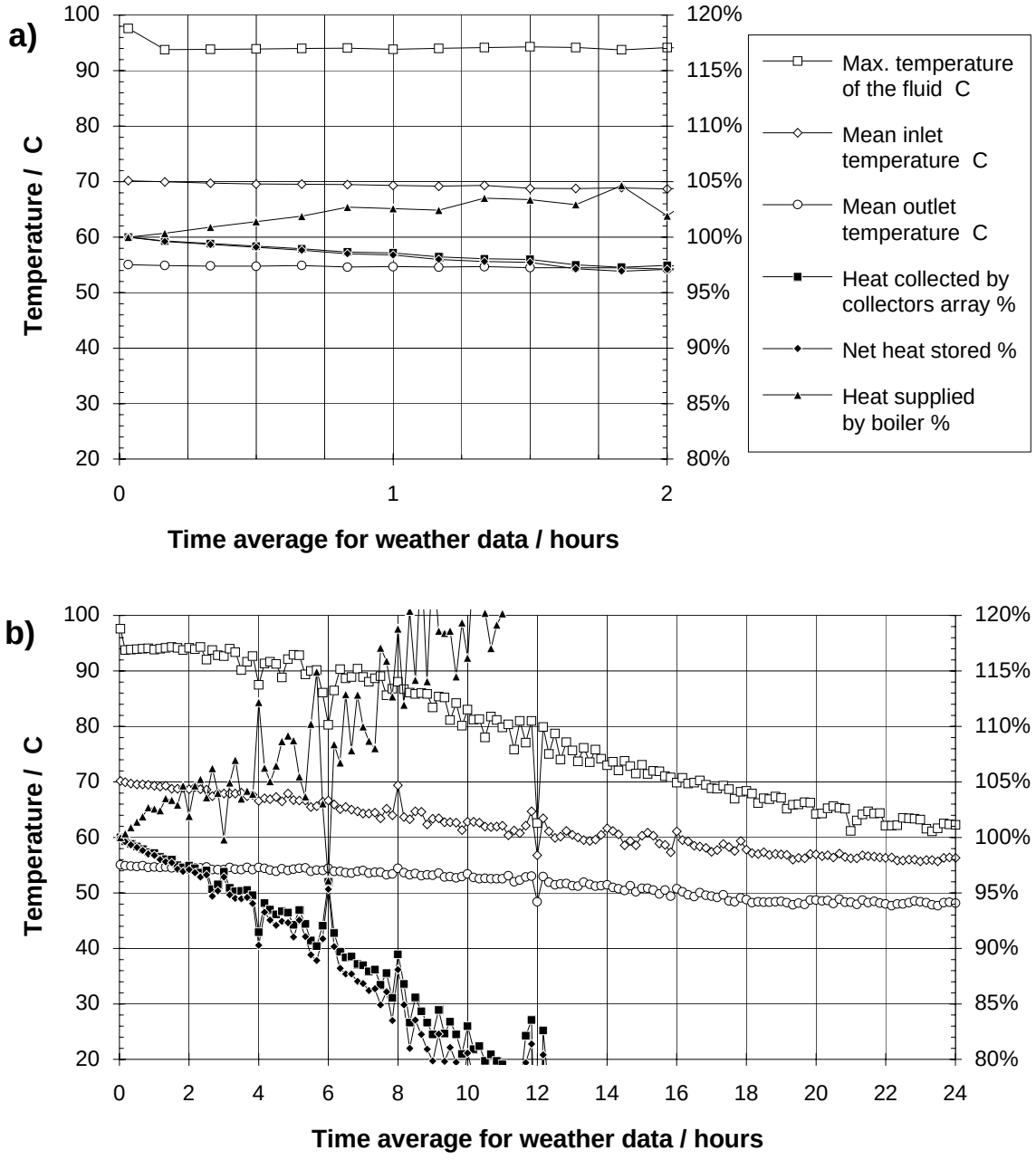

Fig. 3.5 Thermal performances of the reference system, calculated for different time averages of weather data; a) from two-minute up to two-hourly values; b) from two-minute up to daily values.

Temperatures and energies are shown with increasing time scales used to generate mean values of weather data. The energies calculated with the two-minute values are chosen as reference points and set to 100%. Energies calculated with other weather data sets are given as a percentage of their reference value. As expected, the coarser the resolution of the weather data, the larger the deviation of the calculated quantities. The deviation is quite linear up to two-hourly values, and tends to scatter when the length of time-averaged values increases.

Extreme values of parameters were investigated. Their performances were calculated for 32 different sets of system parameters. Combined with the 145 weather data files, about 5'000 simulations were performed. The varied quantities were:

- The store volume (50'000 and 450'000 m^3).
- The ratio between the store volume and the collector area (10 and 20).
- The initial temperature of the store (32 °C and 47 °C).
- The spacing between the boreholes (2.5 m and 4.0 m).
- And the loading flow rates (0.004 and 0.007 kg/m^2s).

All the other parameters were kept to the values given in the reference system. The variation of the store volume (and the collector area in order to keep their ratio constant), changes the importance of the domestic hot water requirement in relation to the size of the solar plant.

The results of the simulations exhibit figures similar to the reference system. Represented graphically as in Fig. 3.5, they show that the use of a weather data file, recorded on a time scale smaller than 2 hours, will not produce great differences in the results. They suggest that a simulation performed with extremely detailed weather values would give similar results. The difference between two-minute and hourly values remains within 2% for the cumulated energies, and 1K for the temperature averages. Only the maximum temperature in the ground heat exchanger may differ by up to 10 K. When the heat capacity of the collector array is included in the programme (see section 3.7), calculations with the reference system show that the difference is reduced to 1 K if the heat capacity is larger than 10 kJ/m^2K.

The use of two-minute weather values rather than longer averaged values has in every case resulted in larger collected and stored monthly energy. With daily weather values, deviations of the monthly collected energy vary between 15 and 40%. In Fig. 3.6, only the differences between the use of hourly and two-minute weather values are shown. The 32 cases are plotted in relation to the extreme values of the 5 investigated system parameters. Sensitivity to the varied parameters is indicated by the lines, as they connect the deviations of two systems whose remaining parameters are identical.

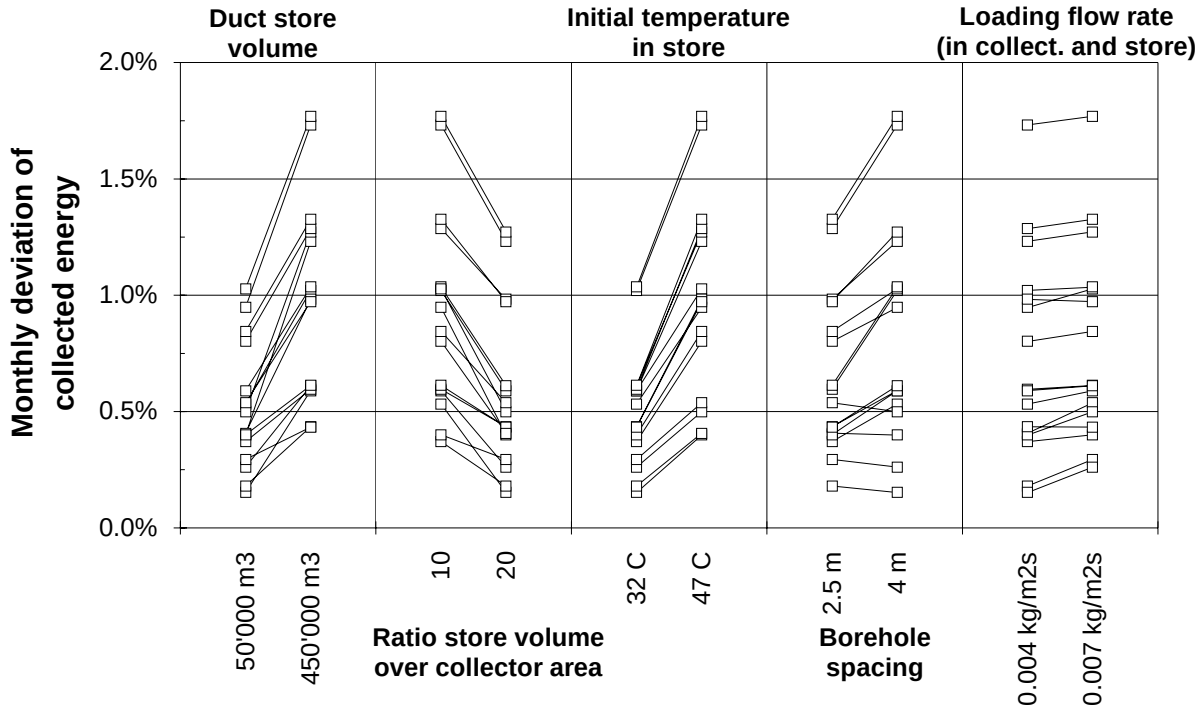

Fig. 3.6 Deviations of the monthly collected energy using two-minute instead of hourly values. The 32 cases are shown in relation to the extreme values of the 5 investigated system parameters.

The largest deviation occurs:

- When the heat delivered to the load (which has a low return temperature), is small in comparison to the heat stored in the duct store.
- When the mean temperature of the duct store is high.
- When the collector area is large in proportion to the duct store volume.
- When the spacing between the boreholes is large.

The variation of the loading flow rate did not give any significant influence. We will see that the deviation increases with any parameter which makes the solar collectors operate at a higher temperature level. The maximum deviation is limited by the maximum allowed fluid temperature in the system.

3.5.2 Parameter Sensitivity

By comparing the results calculated with two-minute and hourly values for the weather data, the sensitivity to some parameters was also investigated. Starting with the reference system, the collector area, store volume, initial temperature of the store and loading flow rates were independently varied. The borehole thermal resistance may be set to a constant value, instead of being calculated. It was also varied in order to cover the range of the most common types of ground heat exchangers.

The flow rate was varied between 0.001 and 0.021 kg/m^{2}K. The calculated energy deviations were reasonably constant and remained below 2%. However, a low flow rate led to higher temperatures of the heat carrier fluid.

The collected and stored energy deviation tends to increase when the ratio *store volume* over *collector area* decreases (see Fig. 3.7). This is not surprising, as the temperature variations between the collector array and the duct store are amplified when this ratio diminishes. A small store volume in the reference system, giving a smaller ratio than 8, leads to an unrealistic system operation, as the temperature of the heat carrier fluid may exceed 100 °C.

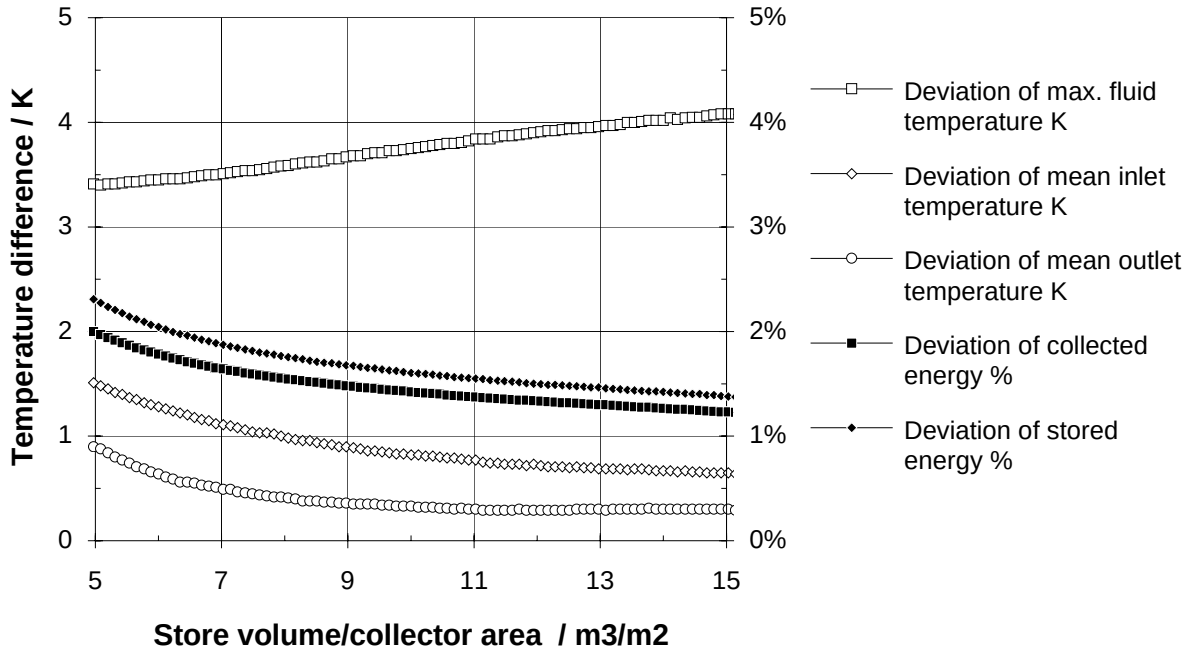

Fig. 3.7 Deviations of the calculated quantities using two-minute instead of hourly values for the weather data. The deviations are shown in relation to the ratio *store volume* over *collector area*. The system parameters are set to the values of the reference system, except the store volume that is varied between 170'000 and 530'000 m^3.

Similar analysis with a larger load (or a smaller store volume and collector area), showed that the collected energy deviation was slightly smaller.

The borehole thermal resistance was varied between 0.01 and 0.20 K/(W/m). The small value corresponds to a very efficient ground heat exchanger, similar to the one calculated in the reference system (open annular duct with turbulent flow). The higher value can represent a double U_pipe inserted into the borehole, with the pipes close to the centre of the borehole and a low thermal conductivity for the filling material (as with bentonite).

The deviations increase with higher borehole thermal resistance and reach about 3% for the collected and stored energy when the resistance is set to 0.20 K/(W/m). Nevertheless, with borehole thermal resistance larger than 0.01 K/(W/m) in the reference system, a water buffer tank is required to prevent water from boiling.

A higher initial temperature in the store also increases the deviation (see Fig. 3.8). The decrease of the collector efficiency with higher temperature is not enough to explain the trend. An initial temperature of 70 °C rather than 30 °C amplifies the absolute deviation by a factor of 3. However, in this case, the initial temperature cannot be higher than 55 °C without leading to an unrealistic system operation.

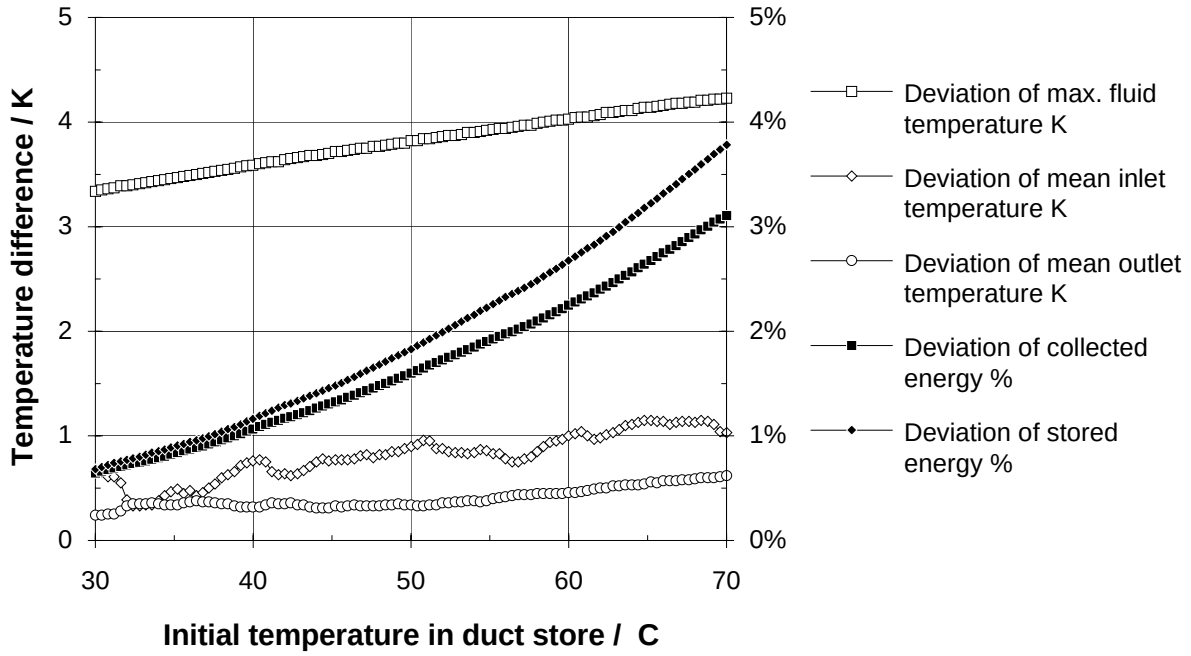

Fig. 3.8 Deviations of the calculated quantities using two-minute instead of hourly values for the weather data. The deviations are shown in relation to the initial temperature of the duct store (beginning of June). The other system parameters are set to the values of the reference system.

A careful examination of the simulated heat rates and fluid temperatures showed that the deviation of the collected energy occurs when the operation of the collector array, simulated with the two-minute weather data values, is interrupted at least once within an hour. For these situations, hourly values of the incident radiation contain periods of time where the incident radiation is too low to operate the collector array. Two effects counteract each other. The collected energy is produced at a lower temperature, enhancing the collector efficiency. On the other hand, the heat rate transferred into the duct store is lower. During these hours, the resulting effect is a lower mean efficiency when simulated with hourly weather data values. These hours occur at the beginning and the end of an operating day, but the contribution to the monthly deviation usually remains small. The monthly deviation is increased by those days whose incident solar radiation exhibits large and fast variations, which fluctuate around the radiation threshold of operation. A higher initial temperature in the store raises the radiation threshold, and, in consequence, the number of hours with part-time operations. One should remember that the simulations have been performed without taking into account the heat capacitive effects of the collector array.

A common feature in the simulated cases is the strong correlation between the mean temperature level in the collectors during operation and the deviation of the monthly collected energy. When the loading flow rates are the same, the monthly deviation can be plotted in relation to the mean fluid inlet temperature into the store during injection (see Fig. 3.9). For all the cases investigated, a realistic system operation (maximum inlet temperature in the duct store below 90 - 100 °C), limits the maximum deviation of the collected energy to 2%. Larger deviations can be expected due to a larger collector loss coefficient, as the maximum fluid temperatures would not rise as much (see section 3.7).

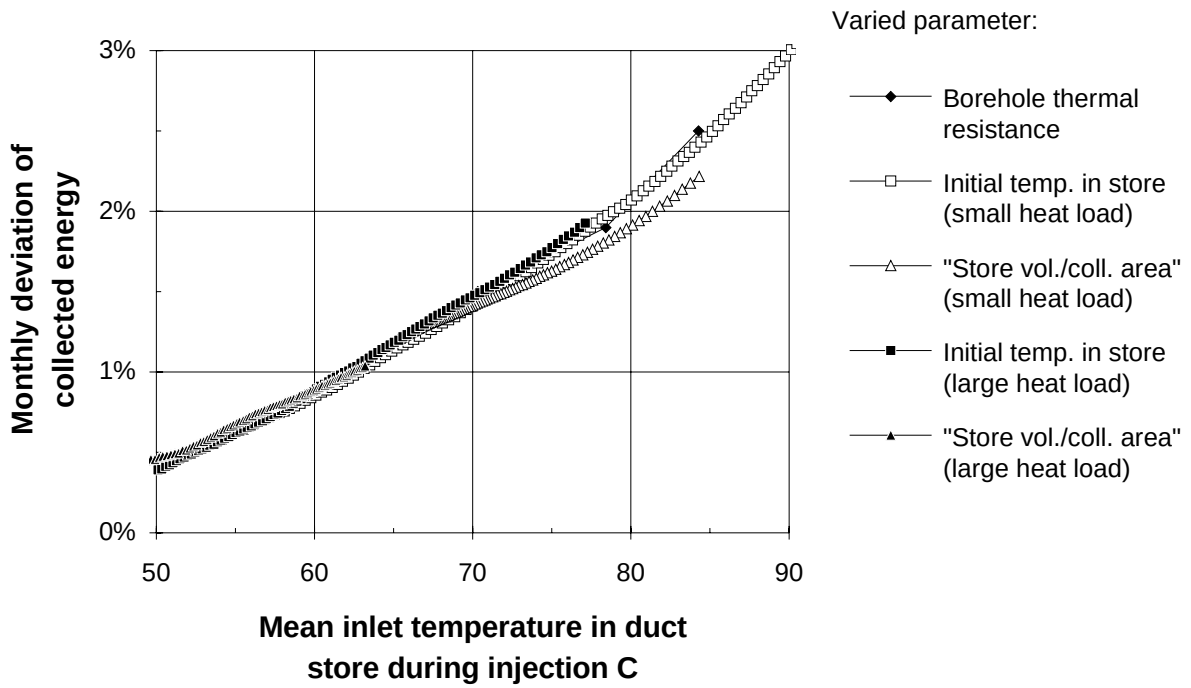

Fig. 3.9 Monthly deviation of collected energy plotted in relation to the monthly mean inlet temperature in duct store during injection (using two-minute weather values). Each curve corresponds to the variation of one parameter.

TRNSYS simulations were performed with the reference system to assess the influence of the system control. Various values of dead-band temperature differences in the collector controller showed that the influence is rather weak, and tends to decrease the deviation of the monthly collected energy.

3.6 System with a Short-Term Buffer Tank

The deviations of the simulated performances using two-minute and hourly weather data have been assessed according to the system design given in section 3.4. An alternative is to add a short-term water buffer tank to this design. Detailed design studies have been performed with such systems [13, 14]. They are similar to the basic design, but differ in the system control. The objective here is to show that the deviations are not increased when a water buffer tank is inserted between the collector array and the duct store. They are calculated for different sets of system parameters, corresponding to the reference system and the three extreme cases found in the previous section: low *store volume* over *collector area* ratio, high initial store temperature and high borehole thermal resistance.

3.6.1 Buffer Tank Model

The water buffer tank is modelled as a stack of equal volumes, or *segments*, of water. The dimensions of a segment are defined by the volume of the buffer tank, its vertical extension and the total number of segments. The vertical temperature profile of the buffer is given by the temperatures of the segments, set to a constant value within each segment. For the same reasons as those given for the duct store (see section 3.2), the heat losses of the buffer tank are not calculated. The inlet and outlet pipes are connected to the top and bottom of the buffer tank (first and last segment). Three hydraulic loops are connected to the buffer; (collector

loop, duct store loop and load loop). The resulting flow rate through the buffer leads to a convective heat transport. Combined with the conductive heat transport between the segments, a new temperature profile is calculated at the end of every time-step. Free convection is dealt with using the established technique [15], by mixing two segments if the temperature of the upper one is lower than the other. Numerical dispersion is not suppressed; a large number of segments are chosen to make it as small as possible (the number of segments is set to 25).

3.6.2 System Design and Operation Strategy used with the Buffer Tank

The water buffer tank is inserted in the system design defined in section 3.4, so that the collector array (via the heat exchanger), the duct store and the load subsystem are directly connected to it. These three subsystems can be operated independently. Two additional pumps are required for the operation of the duct store: one pump when the duct store is loading the buffer; (inlet at the top and outlet at the bottom of the buffer), and the other when the buffer is loading the duct store; (the heat carrier fluid circulates in the opposite direction). The collector array, operated as in the reference system, delivers the collected heat to the top of the buffer. The return flow rate of the load subsystem (the load subsystem is also operated as in the reference system), is injected into the bottom of the buffer. If heat can be transferred from the buffer tank to the duct store, this latter is loaded with a flow rate set to the half of the nominal flow rate in the collectors. If the duct store can load the buffer tank, then the flow rate through the duct store is adjusted to the return flow rate from the load subsystem.

3.6.3 Results with a Buffer Tank in the System

The insertion of a short-term water buffer tank of 5'000 m^3 in the reference system gives the same deviations as the reference system itself (using two-minute and hourly weather data). It should be noted that 6 hours of collector operation are enough to move 5'000 m^3 of heat carrier fluid.

The maximum deviations were found for a low *store volume* over *collector area* ratio of 5 (reference system with twice the collector area), a high borehole thermal resistance of 0.2 K/(W/m) (in the reference system), or a high initial store temperature of 70 °C (in the reference system). These cases led to unrealistic system operation, as the fluid temperature could exceed 100 °C in the duct store. However, the use of a 5'000 m^3 buffer tank makes these cases possible. The deviations are slightly smaller, but in the case of a high initial store temperature of 70 °C (in duct store and buffer tank), the deviation of the monthly collected energy remains close to 3%.

The use of a buffer tank in the system does not increase the monthly deviations. Nevertheless, the range of possible values of system parameters increases. For the extreme cases, the monthly deviations can be larger than for a system without buffer tank. For all the investigated cases, the maximum deviation of the collected energy is limited to 2% for the system design without buffer tank and 3% for the system design with buffer tank.

3.7 Heat Capacity in the Collector Array

The heat capacity of the collector array will smooth the rapid variations of the collected heat rate and fluid temperature. When the incident radiation drops briefly under the radiation threshold for the collection of solar gains, the operation of the collector array will not be interrupted if the resulting fluid temperature variation is sufficiently damped down. The

monthly deviations, using two-minute instead of hourly weather data, are expected to be smaller. In order to confirm this assertion, simulations with a collector heat capacity are performed with the reference system and the extreme cases that led to the maximum deviations in the no-buffer cases.

3.7.1 Collector Model with a Heat Capacity

A one-node model is used to take into account the heat capacity. The collector array is characterised by:

- Its average temperature, defined as the arithmetic mean between the inlet and outlet temperature.
- Its average transmittance-absorptance product, corrected by the collector efficiency factor F'. The incidence angle modifier effects (IAM) are not accounted for.
- Its overall loss coefficient, corrected by the collector efficiency factor F'. The loss coefficient is assumed to be constant.
- A lumped heat capacity, due to the heat carrier fluid and part of the material forming the collectors and pipes.

A heat balance of the collector array is performed for every time-step. The heat exchanger is included in the calculations. The heat balance is expressed in relation to the inlet temperature of the heat carrier fluid on the secondary side of the heat exchanger. When no heat is collected, the temperature of the collector array follows an exponential relaxation toward the outdoor temperature, corrected by a factor which takes into account the absorbed radiation. (This factor, added to the outdoor temperature, is the ratio *absorbed incident radiation* over *loss coefficient*. The time constant of the exponential function is given by the ratio *heat capacity* over *loss coefficient*).

When the heat capacity is set to 0, the one-node model corresponds very well with the model mentioned in section 3.4, provided that the collector flow rate is sufficiently large. This is the case with the parameter values of the reference system (deviation < 0.1%). TRNSYS simulations of the system performed by using the MFC component [16], a collector module with a heat capacity, showed that the one-node model was able to simulate with good accuracy (deviation < 1%) the heat capacitive effects on the monthly collected energy (see chapter 5). (The comparisons were made under the same conditions as those using the standard TRNSYS collector component, see section 3.4.)

3.7.2 Results with a Heat Capacity in the Collector Array

As previously mentioned, a heat capacity of 10 kJ/m^{2}K in the reference system is enough to decrease the difference between the calculated maximum fluid temperatures to about 1 K; (calculations performed with weather data of two-minute and hourly values). The deviations related to the other calculated quantities are also slightly decreased.

The effect of the heat capacity is greater with the extreme figures shown in section 3.5; (low *store volume* over *collector area* ratio of 5, high borehole thermal resistance of 0.2 K/(W/m) or high initial store temperature of 70 °C). The deviation of the collected energy, (which could attain 3%), remains below 1.5% when a heat capacity of 10 kJ/m^{2}K is used. The heat capacitive effects are illustrated in Fig. 3.10, for the case of a high initial store temperature (70 °C) in the reference system. The collected heat rate and the outlet fluid temperature on the secondary side of the solar heat exchanger are plotted on a two-minute basis. They are shown for three different values of the collector heat capacity (0, 10 and 20

kJ/m^{2}K). The time constant of the collector array (see below) is also indicated. In order to highlight the interruptions in the collection of solar gains in Fig. 3.10, the fluid temperature is drawn as being set to zero when the collector pump is off. The curves represented by thin lines are calculated using two-minute values for the weather data, and the thick ones using hourly values.

When the collector heat capacity is not accounted for, the monthly collected energy deviation is 3.1% and the largest daily contribution occurs the 14 of June. (The corresponding incident radiation is shown in Fig. 3.1 on a two-minute basis.) For this day, the collected energy is overestimated by 9.3% when two-minute values are used instead of hourly weather data, due to the predominance of part-time operation in one case and not in the other. With a collector heat capacity of 10 kJ/m^{2}K (respectively 20 kJ/m^{2}K), the monthly deviation drops to 1.4% (respectively 1.1%). For the 14th of June, the deviation drops to 1.3% (respectively 1.0%). If the collectors are operating without interruption for a whole hour, using two-minute or hourly weather data, the difference in the collected energy or the mean fluid temperature is negligible. The warming up of the collector array is illustrated in Fig. 3.10, as the collector operation starts later when the collector heat capacity is larger. For that day, the collected energy, simulated with hourly weather data, is reduced by respectively 2.3% and 5.9%, with a heat capacity of respectively 10 kJ/m^{2}K and 20 kJ/m^{2}K.

If the heat capacity of the collector array is not accounted for, a larger collector loss coefficient leads to a larger monthly deviation of the collected energy. This is due to the raised radiation threshold for the collection of solar gains, the decreased collector efficiency and the increased range of possible parameter values. Simulations with the reference system and the extreme cases that led to the maximum deviations (in the no-buffer case), were performed with a collector loss coefficient of 5 instead of 3.5 W/m^{2}K. (A collector loss coefficient of 5 W/m^{2}K at high temperature is considered to be an extreme value for a collector array that is expected to operate at high temperature). The largest deviation reached nearly 6%, but was decreased to 2% with a heat capacity of 20 kJ/m^{2}K. In order to understand how the collector array will smooth the incident radiation, a better criterion is given by the time constant of the collector array. It is defined by the ratio between its *total heat capacity* and its *total heat loss factor* (collector + piping). For all the investigated cases, the deviation was small (below 2%), provided that the time constant was larger than about 1 hour. In other words, the collector array behaves so that the rapid variations of the incident radiation are integrated. It has approximately the same effect as integrating the measured radiation to produce hourly values. This criterion is usually met by most of today's collector arrays that are designed to operate at high temperature.

With the case presented in Fig. 10, the largest contribution to the monthly deviation of the collected energy occurs the 14th of June. On that day the daily deviation reaches nearly 10%. The daily deviation tends to increase with decreasing daily incident insolation, but its contribution to the monthly deviation decreases. Similarly the monthly deviation is expected to be larger in winter, but the contribution to the annual deviation is assumed to be small, especially if the heat capacitive effects of the collector array are taken into account. In winter-time the interactions between the load and the store dominate those between the collector array and the store. The load variations are rather smooth, in particular due to the heat capacitive effect of the buildings that integrate the variations of the meteorological variables. The fast variations of the domestic hot water demand are usually smoothed by a short-term water tank. For these reasons the case-study performed is considered to be the worst situation. The annual deviation of the system performances, using hourly instead of two-minute weather values, should not exceed the limits found with the case-study.

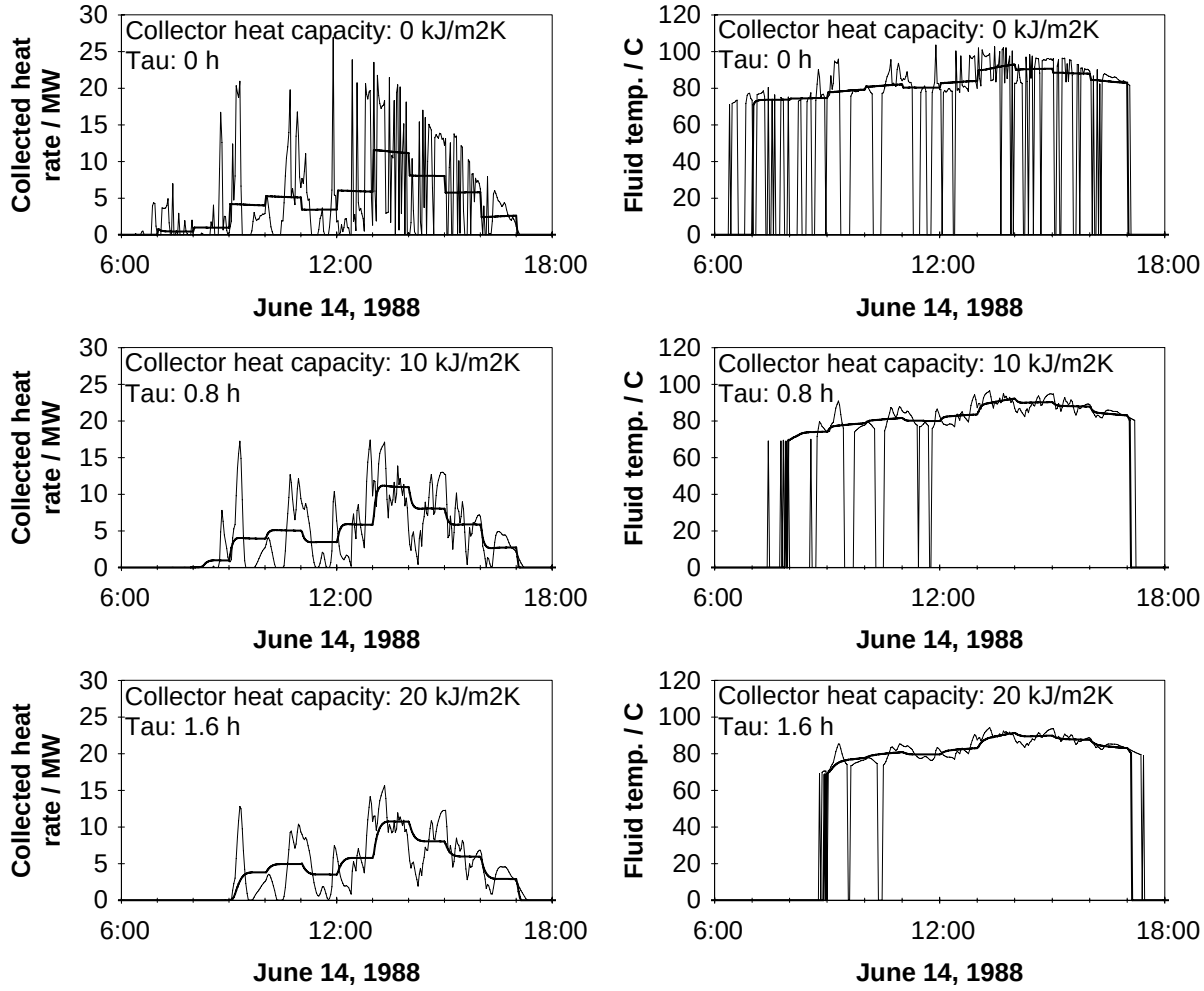

Fig. 3.10 Evolution of the collected heat rate and the outlet fluid temperature on the secondary side of the solar heat exchanger. The curves are simulated with the reference system, a high initial store temperature (70 °C) and three different values of the collector heat capacity. The thin ones are calculated using two-minute weather values and the thick ones using hourly values.

3.8 Conclusion

The effect of the weather data time-step on the overall performances of a commonly used system design with a seasonal duct store has been assessed. This study was primarily aimed at testing the validity of the duct store model. A typical solar energy system, designed to be operated at medium or high temperature, was defined and used to perform a case-study. System simulation programmes, based on the system design, were developed to compute in great detail the local solutions in the duct store. Other versions were created to simulate the influence of a short-term buffer tank added to the system, or the heat capacitive effects of the collector array.

The common use of hourly rather than two-minute weather data values results in a slight deviation in the global simulated performances. For a typical summer month (June), the cumulated energies (collected and stored) are always smaller, but the deviation is limited to 2%. The mean temperatures of the heat carrier fluid differ by a maximum of 1 K.

Larger deviations can occur when a buffer tank is added to the system, due to a larger range of possible parameter values, or when a poor collector array is used. If the heat capacity of the collector array is taken into account, the deviations are decreased to the previous limits, provided that the time constant of the collector array is larger than about one hour.

We conclude that it is quite reasonable to use hourly meteorological data values in order to perform detailed simulations of a solar heating system using a duct store. Nevertheless, the maximum established deviations (2% on cumulated energies and 1 K on mean temperatures), give an indication of the most precise results that a simulation can achieve.

4. SIMULATION OF A SOLAR ENERGY SYSTEM WITH A SEASONAL DUCT HEAT STORE IN THE GROUND

4.1 Introduction

Extensive studies of central solar heating plants with seasonal storage (CSHPSS) are usually performed with the help of a system simulation programme. The subsystems and system layout can be built into the programme, as in MINSUN [1], or left to the specification of the user, as in TRNSYS [2]. MINSUN and TRNSYS have the required component models that simulate the main subsystems of a CSHPSS. The seasonal storage models have been developed at Lund university [3,4,5] and adapted to create storage components for each of the two programmes [6,7,8,9]. Detailed design studies of central solar systems with duct store have been performed with the TRNSYS programme [10,11] (CSHPSS system using a short-term water buffer tank). Other studies have been carried out with the MINSUN programme [12] or SAESONSOL, a Danish-used programme [13,14].

The considered CSHPSS-systems are based on the system designs described in chapter 3 (system with or without buffer tank). These systems are designed to operate at medium or high temperature without a heat pump. Solar heat is collected through flat plate collectors and stored in a ground heat rock store. Heat is delivered to the consumer through a distribution network.

Simulations of a solar energy system with a duct store sometimes neglect the heat capacitive effects of the collector array. Concerning the duct store, heat capacitive effects of the fluid in the ground heat exchanger are usually not taken into account; furthermore, the heat transfer from the fluid to the ground in the immediate vicinity of the duct (or borehole) is often calculated with a constant heat transfer resistance [4]. The use of a solar source coupled to a duct store sometimes results in large variations of the fluid temperature in the collector array and the ground heat exchanger during the day. Heat capacitive effects related to these temperature variations may have some influence on the heat balance of the system. In the ground heat exchanger, the fluid temperature and the flow rate, in addition to daily variations, usually greatly differ between a summer loading period and a winter unloading period. The heat transfer resistance from the fluid to the ground in the immediate vicinity of the duct (or borehole), which depends on flow conditions, may significantly vary.

The reference system defined in chapter 3 is used to perform a case-study. The objective is to assess the magnitude of the different effects previously mentioned for typical solar energy systems using a duct store (with or without short-term buffer tank).

4.2 Methodology, System Design and Simulation Programmes

Simulations are performed for a typical summer month (June), with weather data measured at Nykvarn, a northern location at 59.2° latitude (see chapter 3 for additional information). Hourly weather-data values are used, as an hourly time-step in the representation of the weather data does not significantly affect the simulated thermal performances of the system (see chapter 3).

The two simulated system designs are shown in Fig. 4.1 and 4.2. (See chapter 3 for the description and operation strategy of the systems.) The reference system defined in chapter 3 (without buffer tank), is chosen for the case-study.

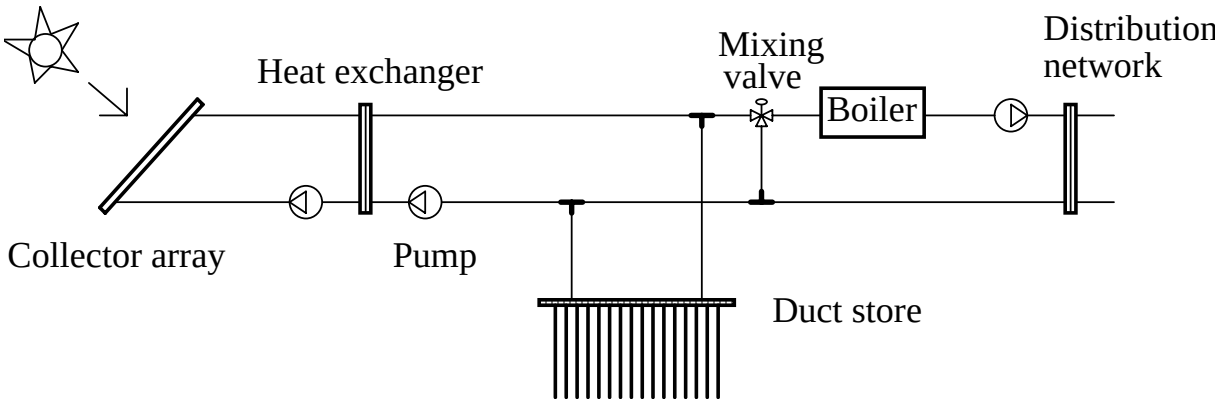

Fig. 4.1 Design of the system without buffer tank.

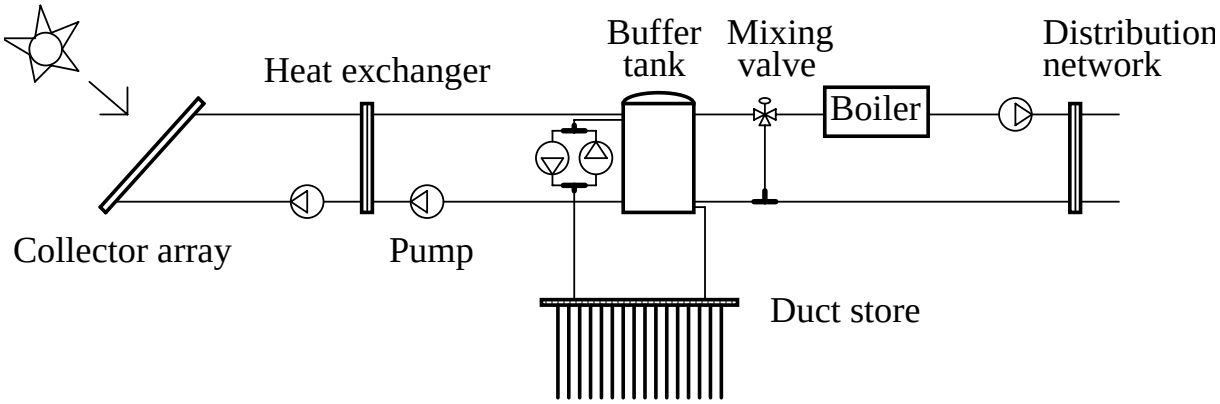

Fig. 4.2 Design of the system with buffer tank.

The system performances are simulated with the help of the detailed programmes described in chapter 3. Eight different versions of the programme exist, as the following features are or are not simulated:

- the heat capacitive effects related to the collector array;
- the heat capacitive effects related to the ground heat exchanger;
- the use of a short-term buffer tank in the system.

The versions can be adapted so that the simulation results may be compared with TRNSYS systems using the duct store component (DST). (The borehole thermal resistance is set to a constant value and the vertical division of the store is reduced to 1 cell. See chapter 5 for comparisons).

Heat capacitive effects in the collector array and the ground heat exchanger are assessed separately. The effects are shown by comparing the simulated monthly collected energy with the value obtained when no heat capacity is taken into account in the collector array and the ground heat exchanger.

4.3 Heat Capacitive Effects in the Collector Array

Heat capacitive effects in the collector array result in a decrease of the collected energy. The decrease depends on the operation temperature level of the collector array and the value of the heat capacity that characterises the collector array. The heat capacity is essentially imputed to the fluid in the collector loop and part of the material affected by the heating of the collector array (collectors, pipes, etc.). Most of the effect is due to the pre-heating of the collector loop before usable solar gains are collected. The collector array of a central solar plant with a duct store, which is designed to operate at medium or high temperature, will operate most of the time at high temperature.

In Fig. 4.3, the decrease of the collected energy, simulated using the reference system with or without a 5'000 m^3 buffer tank, is shown for various values of heat capacity in the collector array.

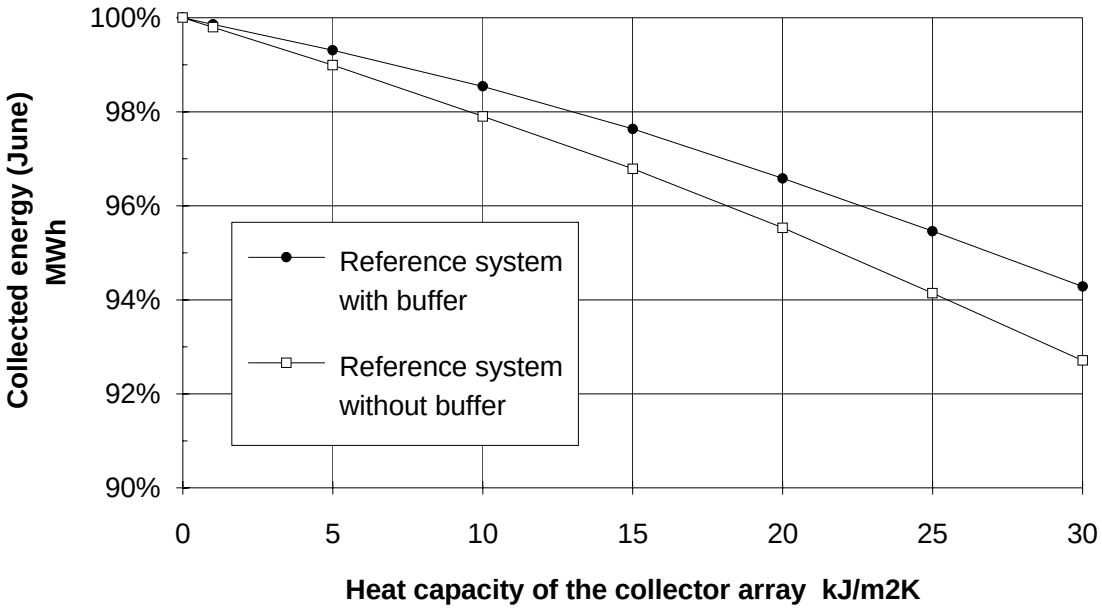

Fig. 4.3 Heat capacitive effects simulated using the reference system with or without a 5'000 m^3 buffer tank (month of June).

In Fig. 4.3, the decrease of the collected energy is simulated for one summer month (June). In order to assess the global effect on the annual heat balance of the system, a simulation with at least one year of weather data is required. This is realised with a TRNSYS system based on the system design given in Fig. 4.1 (system without buffer tank; see chapter 5). TRNSYS simulations performed with the reference system during 20 years (including the transient heat losses of the duct store) showed a global collected energy decrease of 2.5%, 6.0% and 9.5% with heat capacity of respectively 10, 20 and 30 kJ/m^2K in the collector array.

These examples indicate that the collected energy decrease can be significant for heat capacity values larger than 10 kJ/m^2K in the collector array. The use of a collector component that includes heat capacitive effects is then recommended for accurate simulations. A special collector component, based on the Matched Flow Collector model [15] has been developed to

be used in TRNSYS. This collector model takes into account heat capacitive effects as well as a quadratic temperature dependence of the overall loss coefficient.

4.4 Heat Capacitive Effects in the Ground Heat Exchanger

The heat capacitive effects in the ground heat exchanger are beneficial to the collection of solar gains. The injection of intense but variable heat rates in the duct store results in large and rapid variations of the fluid temperature in the ground heat exchanger. The heat capacity of the fluid and borehole material tends to smooth the temperature variations and thus the net heat rate transferred to the ground. In consequence the mean temperature level of the fluid is lower than that which would be simulated without heat capacity, resulting in better collector efficiency.

In the reference system, the heat capacity of the ground heat exchanger is relatively important as most of the volume of the boreholes is filled with water (open annular ducts). The volume of water equals 420 m^3, or 12 litres per square meter of collector area, representing 0.2% of the store heat capacity. In Fig. 4.4, the heat capacitive effects on the collected energy are shown for different values of borehole thermal resistance and initial store temperature in the reference system. Simulations are performed for the month of June. The range of variations of the borehole thermal resistance covers the values of the most common types of ground heat exchangers. The maximum possible difference is limited by the maximum temperatures allowed in the different subsystems. At the most, the inlet fluid temperature in the duct store must not exceed 100 °C. If this occurs, the differences in Fig. 4.4 are plotted with black squares joined with a plain line; otherwise, white squares and dotted lines are used.

With the reference system, the heat capacitive effects in the ground heat exchanger can be important with a high borehole thermal resistance (10% increase of the collected energy in June). Nevertheless, a realistic operation of the system at high temperature (up to 60-70 °C in the duct store), requires an extremely low borehole thermal resistance, reducing the maximum possible difference to below 1%.

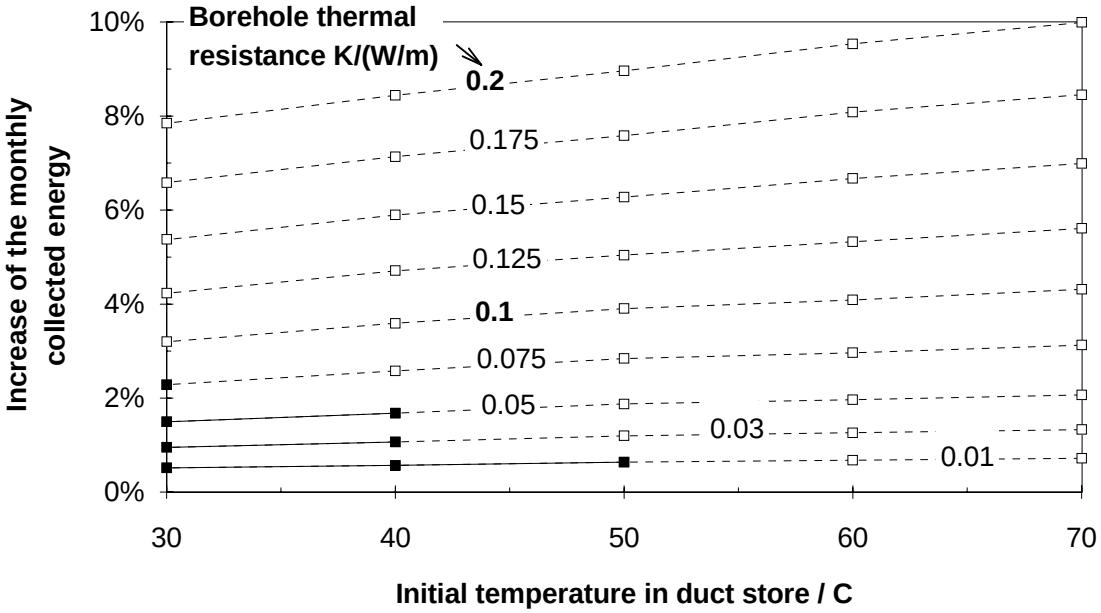

Fig. 4.4 Increase of the monthly collected energy (June) when heat capacitive effects in the ground heat exchanger are taken into account. The reference system is used for the simulations. If the inlet fluid temperature in the duct store remains below 100 °C, the differences are plotted with black squares.

Relatively to the system design without buffer tank, the most significant parameters that affect the heat capacitive effects in the ground heat exchanger are:

- borehole heat capacity and thermal resistance;
- ratio between the collector area and the total borehole length;
- thermal characteristics of the collector array (transmitttance-absorptance product, overall loss factor and heat capacity);
- and thermal characteristics of the ground (thermal conductivity and thermal diffusivity).

In order to permit a higher borehole thermal resistance in the reference system, some parameters were independently varied. The spacing between the boreholes was reduced from 3 to 2.5 m (total borehole length increased by 40%), the thermal conductivity of the ground was increased from 3.5 to 4.5 W/mK and the collector area was reduced from 35'000 to 17'500 and 11'700 m^2 (the ratio *collector area* over *store volume* was increased from 10 to 20 and 30). All these variations result in smaller heat capacitive effects. Nevertheless, the largest possible difference is obtained when the collector area is reduced to 11'700 m^2. A borehole thermal resistance of 0.2 K/(W/m) still leads to a realistic system operation. In this case, the maximum difference is increased to 4%. However a system with a *store volume* over *collector area* ratio as high as 30 is not likely to operate at medium or high temperature.

A parameter that has not been varied so far is the overall loss coefficient of the collector array. A value of 3.5 W/m^2K at high temperature, as in the reference system, represents an excellent collector array (using flat plate collectors). On the other hand, a value of 7 W/m^2K characterises a poor collector array if designed to operate at high temperature. Such a value in the reference system makes the use of a ground heat exchanger with a high borehole thermal resistance possible. The decrease of the collector efficiency, due to its higher overall loss

coefficient, increases the importance of the heat capacitive effects in the ground heat exchanger. In Fig. 4.5, they are shown for an overall loss coefficient of 7 W/m^{2}K and a collector area of 50'000 m^2 in the reference system (*store volume* over *collector area* ratio of 7). For this extreme case, the maximum possible difference can reach 15% of the collected energy.

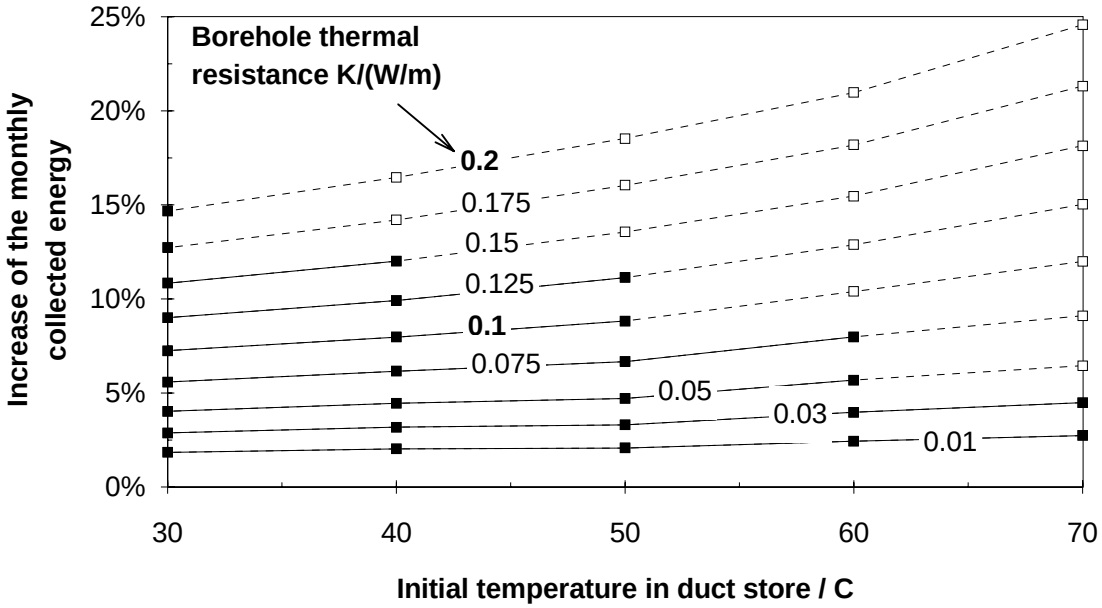

Fig. 4.5 Increase of the monthly collected energy (June) when heat capacitive effects in the ground heat exchanger are taken into account. The overall loss coefficient and area of the collector array are respectively set to 7 W/m^{2}K and 50'000 m^2 in the reference system. If the inlet fluid temperature in the duct store remains below 100 °C, the differences are plotted with black squares.

A short-term buffer tank, inserted between the collector array and the duct store, reduces the heat capacitive effects in the ground heat exchanger. In Fig. 4.6, they are shown in relation to the size of the buffer tank which is added to the reference system. In order to obtain similar fluid temperatures between the reference system with or without a small buffer tank, the flow rate through the duct store equals that of the collector array when the duct store is loaded by the buffer tank. A smaller loading flow rate in the duct store decreases the differences. When it is halved, the maximum difference lies between 6 and 8% instead of 8 to 10%.

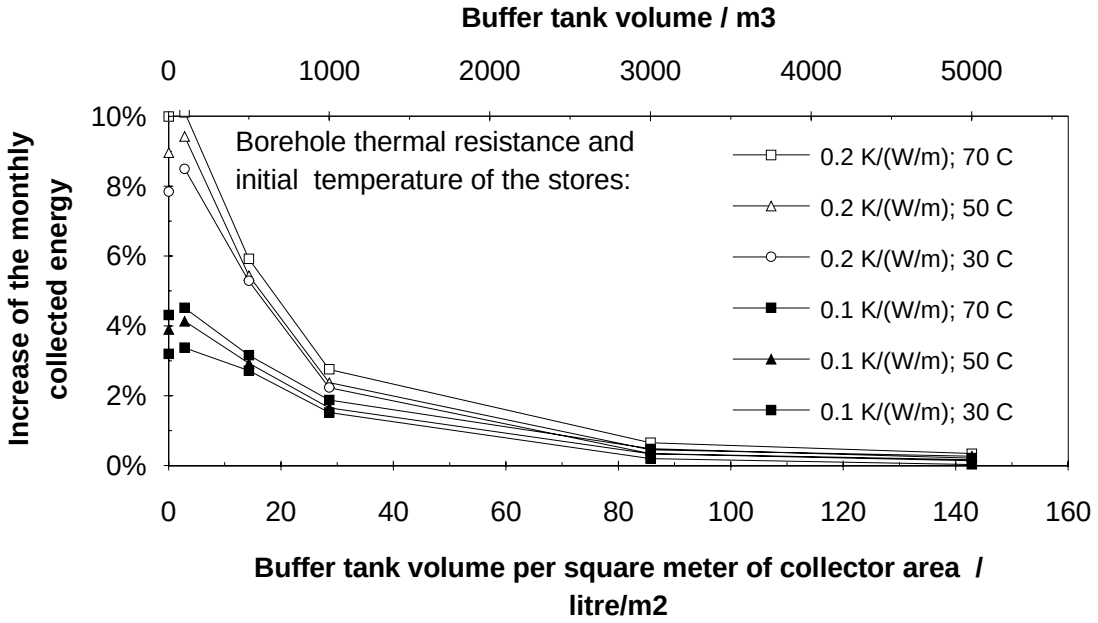

Fig. 4.6 Increase of the monthly collected energy (June) when heat capacitive effects in the ground heat exchanger are taken into account. The differences are plotted in relation to the size of the buffer tank which is added in the reference system. They are shown for various values of borehole thermal resistance and store temperature.

The maximum possible difference remains below 1% if the duct store temperature is expected to exceed 50 °C. Simulations with the previous extreme case (overall loss coefficient and area of the collector array set to 7 W/m^{2}K and 50'000 m^2), showed that the maximum possible difference was reduced to 6% with a buffer tank of 1'000 m^3 (or 20 litres/m^2 of collector area) and remained below 2% with a 3'000 m^3 buffer tank (or 60 litres/m^2 of collector area).

If the heat capacity of the collector array is taken into account in the simulations, the simulated heat capacitive effects in the ground heat exchanger are reduced. The reduction depends on the time constant of the collector array, defined as the ratio between its *total heat capacity* and its *total heat loss factor*. A collector heat capacity of 10, 20 and 30 kJ/m^{2}K in the reference system gives a time constant of respectively 0.8, 1.6 and 2.4 hours. The maximum increase of collected energy (10% with the reference system), is reduced respectively to 8, 6.4 and 4.9%. With the extreme case, the reduction is smaller as the overall loss coefficient is twice as large, halving the time constant of the collector array (with the same heat capacity). The maximum increase of collected energy, simulated at 24.6% without collector heat capacity, is reduced to 21.4, 19.0 and 17.6% with heat capacity of respectively 10, 20 and 30 kJ/m^{2}K. When a buffer tank is added to this extreme system (larger than 500 m^3), the heat capacity of the collector array has practically no influence on the heat capacitive effect in the ground heat exchanger. The heat capacity of the collector array tends to smooth the temperature variations of the fluid, thus reducing the heat capacitive effects of the ground heat exchanger. However this effect is dominated by a buffer tank having a sufficiently large volume.

4.5 Computation of the Local Solutions in the Duct Store

Precise simulations with a duct store require, in particular, accurate computations of the heat transfers along the flow path, from the fluid to the ground in the immediate vicinity of the boreholes. These computations are performed with the local solutions, which should take into account the following thermal processes:

- a varying fluid-to-ground thermal resistance, due to the variations of the flow rate and fluid temperature;
- the heat transfers between the downward and upward fluid channels in the borehole, due to a varying fluid temperature along the flow channels.

Furthermore, the local solutions should account for a connection in series of the boreholes, as well as a vertical division of the store volume. The heat capacitive effects of the ground heat exchanger can be neglected, provided that a sufficiently large buffer tank (> 60 litres/m^2 of collector area) and/or a performant collector array are used.

The variation of the fluid-to-ground thermal resistance is particularly important with a ground heat exchanger formed by open annular duct [16]. Detailed computations of these effects are given by Hellström [17] for all of the most common types of ground heat exchanger.

The heat transfer between the downward and upward fluid channels in the borehole can be significant with a deep store (> 100 m) and a low flow rate (< 0.5 m^3/h per borehole). This phenomenon can be computed using the concept of effective fluid-to-ground thermal resistance [17]. The vertical temperature profile along the borehole wall should be known. Analytical solutions have been worked out for two basic cases [17]. The first one assumes a uniform heat flux along the borehole and the second a uniform wall temperature along the borehole. The analytical expressions for the effective fluid-to-ground thermal resistance are:

Uniform heat flux along the borehole:

$$R_b^{*q} = R_b + \frac{1}{3} \cdot \frac{1}{R_a} \cdot \frac{H^2}{(C_f\ V_f)^2} \qquad (4.1)$$

R_b: local fluid-to-ground thermal resistance [K/(W/m)];
R_a: overall thermal resistance between the upward and downward fluid [K/(W/m)];
H: active length of the borehole [m];
V_f: fluid flow rate in the borehole [m^3/s];
C_f: volumetric heat capacity of the fluid [J/m^3K].

Uniform wall temperature along the borehole:

$$R_b^{*T} = R_b \cdot \eta \cdot \coth(\eta) \tag{4.2}$$

where

$$\eta = \frac{H}{C_f \, V_f} \; \frac{1}{2 \, R_b} \; \sqrt{1 + 4 \, \frac{R_b}{R_{12}^{\Delta}}} \tag{4.3}$$

See formula (4.1) for the signification of the symbols;

R_{12}^{Δ}: thermal resistance between the upward and downward fluid, when the heat transfer resistances are represented with a Δ-circuit between the upward fluid, the downard fluid and the borehole wall [K/(W/m)];

For a coaxial pipe installation (annular duct):

$$R_{12}^{\Delta} = R_a \tag{4.4}$$

For a U-pipe installation, assuming a symmetrical position of the pipes:

$$R_{12}^{\Delta} = \frac{4 \, R_b \, R_a}{4 \, R_b - R_a} \tag{4.5}$$

Simulations with a 5'000 m^3 buffer tank in the reference system permit an assessment of the effect of the heat transfer between the downward and upward fluid channels in the borehole (coaxial installation). When the heat capacitive effects in the ground heat exchanger are simulated, all the heat transfers in the borehole are calculated, including the heat exchange between the upward and downward fluid channel. This is not the case when heat capacitive effects are not taken into account; in this case only the borehole thermal resistance is calculated. The heat exchange between the upward and downward fluid channel is neglected. A direct comparison of the collected energy simulated by both these versions is possible, as the heat capacitive effects in the ground heat exchanger are negligible with a 5'000 m^3 buffer tank in the reference system.

In table 4.1, the monthly collected energy and net heat stored in the duct store are presented. The loading flow rate in the duct store is decreased by changing the loading strategy. The duct store is loaded with, respectively, 1, 1/2, 1/4 and 1/8 of the collector flow rate. The monthly energies are simulated with 4 different computations of the local solutions:

- all the heat transfers in the borehole are calculated, including heat capacitive effects. The simulated energies with these local solutions are used as reference values;
- the heat rate transferred to/from the ground is calculated with the local fluid-to-ground thermal resistance (R_b);
- the heat rate transferred to/from the ground is calculated with the effective fluid-to-ground thermal resistance (R_b^{*T}), assuming a uniform wall temperature along the borehole;

- the heat rate transferred to/from the ground is calculated with the effective fluid-to-ground thermal resistance (R_b^{*q}), assuming a uniform heat flux along the borehole.

Simulations: month of June		Computation of the local solutions:							
Loading strategy in duct store:		detailed MWh	diff	with R_b MWh	diff	with R_b^{*T} MWh	diff	with R_b^{*q} MWh	diff
Vcoll (2.5 m^3/h /bore)	C:	2'341	-	2'347	+0.3%	2'317	-1.0%	2'342	+0.0%
	S:	1'959	-	1'967	+0.4%	1'933	-1.3%	1'961	+0.1%
Vcoll/2 (1.2 m^3/h /bore)	C:	2'351	-	2'374	+1.0%	2'317	-1.4%	2'355	+0.2%
	S:	1'959	-	1'988	+1.5%	1'920	-2.0%	1'965	+0.3%
Vcoll/4 (0.6 m^3/h /bore)	C:	2'292	-	2'348	+2.4%	2'243	-2.1%	2'289	-0.1%
	S:	1'874	-	1'940	+3.5%	1'816	-3.1%	1'871	-0.2%
Vcoll/8 (0.3 m^3/h /bore)	C:	2'115	-	2'193	+3.7%	2'049	-3.1%	2'103	-0.6%
	S:	1'650	-	1'746	+5.8%	1'569	-4.9%	1'636	-0.8%

Table 4.1 Simulated collected (C) and net stored (S) energy with a 5'000 m^3 buffer tank in the reference system. "Vcoll" is the flow rate of the collector array. The local solutions are computed with 4 different approaches. They show the effect of a varying temperature along the flow channels. (The ground heat exchanger is formed by open annular ducts.)

The effective fluid-to-ground thermal resistance derived from a uniform heat flux along the borehole is the most suitable in this case. It reproduces the heat transfers in the duct store that lead to the collected and stored energies, simulated with the detailed computation of the local solutions. In addition to the local fluid-to-ground thermal resistance, only the thermal resistance between the upward and downward fluid has to be computed.

This correlation has been obtained with a ground heat exchanger formed by open annular ducts. A solar heating system was simulated during a typical summer month (the reference system), and a large water buffer store was used (140 liter/m^2 of collector) to minimise the heat capacitive effects of the ground heat exchanger.

For further investigations, the programmes were modified to support a U-pipe installation in addition to a coaxial pipe installation. A simple situation was simulated to reduce the heat capacitive effects of the ground heat exchanger: the duct store of the reference system is heated with a constant inlet temperature in the ground heat exchanger. The thermal characteristics of the coaxial pipe or the U-pipe installation were varied to cover a wide range of ground heat exchangers, as was the flow rate, set to a constant value for each simulation. The injected heat after 1 month of operation, simulated by using the different methods for the computation of the local solutions, was used for the comparisons. When the ground heat exchanger consists of coaxial pipes, a uniform heat flux along the boreholes is representative for large fluid flow rates, whereas a uniform wall temperature is more suitable for low flow rates. With U-pipes installations, a uniform wall temperature is appropriate for the whole range of flow rates. See Fig. 4.7 for two comparison examples, one performed with a coaxial pipe and the other with a U-pipe installation.

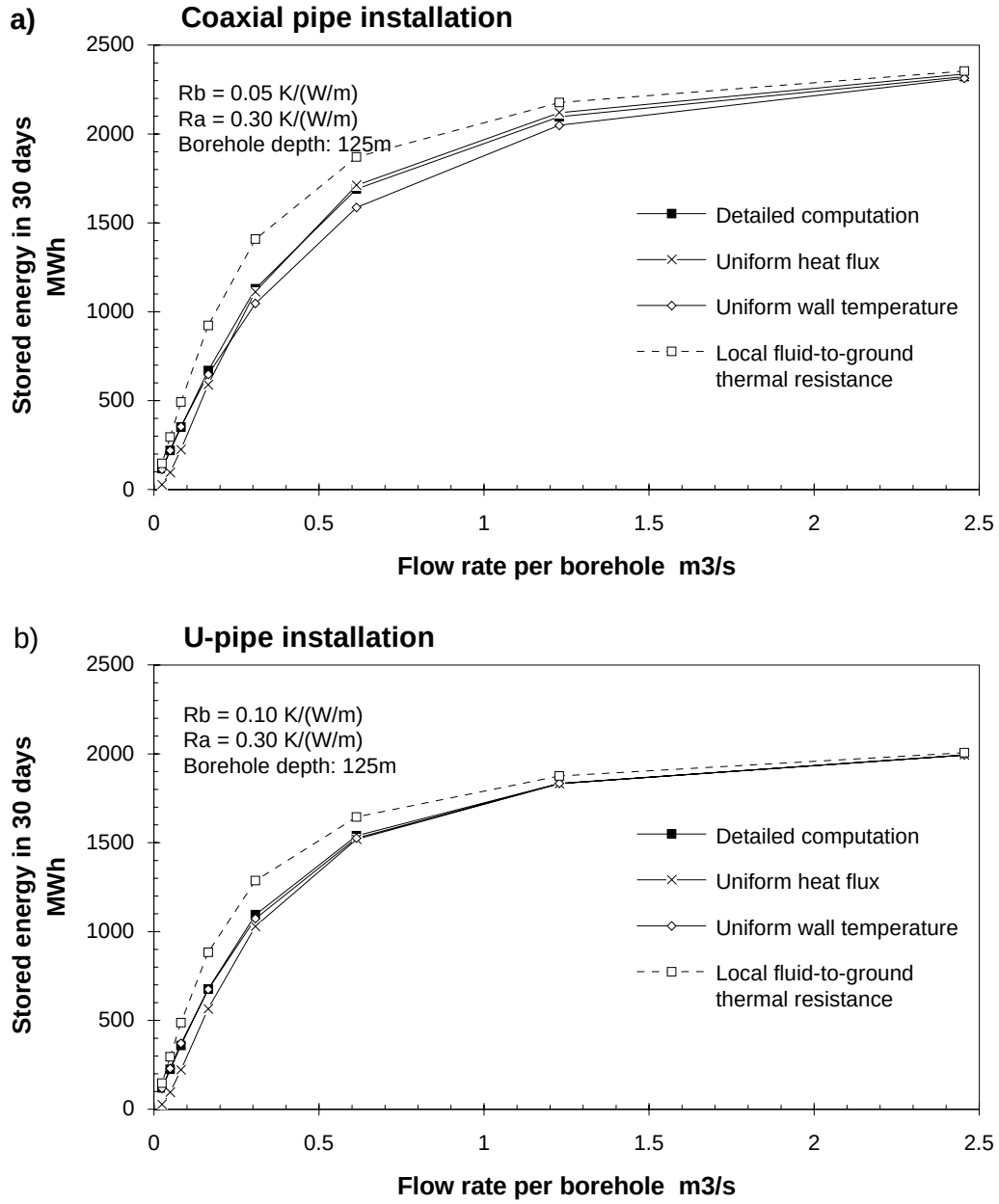

Fig. 4.7 Counterflow heat exchange between the ducts: a detailed description of the heat exchange within the boreholes, the concept of effective fluid-to-ground thermal resistance for a uniform heat flux as well as for a uniform wall temperature along the boreholes, are used to simulate the injected energy in a duct store. The local fluid-to-ground thermal resistance alone is also used to show the difference with a more precise computation. The heat quantities are plotted in relation to the flow rate per borehole, set to a constant value for each simulation. In Fig. 4.7a, a coaxial pipe installation is simulated. A uniform heat flux is representative for large fluid flow rates, whereas a uniform wall temperature is more suitable for low flow rates. In Fig. 4.7b, a U-pipe installation is simulated. A uniform wall temperature is appropriate for the whole range of flow rates.

With the coaxial pipe installations, the borehole thermal resistance R_b was varied between 0.01 and 0.20 K/(W/m), and the overall thermal resistance between the upward and downward fluid R_a was decreased from a very large value down to 0.1 K/(W/m). With the U-pipe installations, R_b was varied between 0.05 and 0.2 K/(W/m) and R_a between 2 and 3 times R_b. For all the cases and the whole range of flow rate values, the correspondence between the detailed simulations and those using the effective fluid-to-ground thermal resistance is satisfactory. With coaxial pipes, the distinction between a uniform heat flux and a uniform wall temperature along the borehole is given by the smallest effective resistance value calculated for both cases.

4.6 Conclusion

Some phenomena related to the simulation of a CSHPSS-system with a duct store were addressed. The heat capacitive effects in the collector array or the ground heat exchanger were assessed for typical solar energy systems, designed to operate at medium or high temperature. Detailed system simulation programmes were used to simulate the different effects. The local solutions in the duct store were computed according to various approaches.

Some simulations over 20 years showed a decrease of the collected energy of 2.5%, 6.0% and 9.5%, with heat capacity values of respectively 10, 20 and 30 kJ/m^{2}K in the collector array. They suggest that the heat capacitive effects should be taken into account for values larger than 10 kJ/m^{2}K.

The heat capacitive effects of the ground heat exchanger, simulated for a typical summer month (June), can significantly enhance the mean collector efficiency in some extreme cases. These effects usually remain small. They can be neglected, provided that a sufficiently large buffer tank (> 60 litres/m^2 of collector area) and/or a performant collector array are used (collector loss coefficient of 3-4 W/m^{2}K at high temperature).

The local solutions in the duct store require special care when computed. In order to perform accurate simulations and proper sensitivity analysis, the fluid-to-ground thermal resistance should depend on the flow conditions. The axial effects, due to a varying fluid temperature along the flow channels, are taken into account with the concept of effective fluid-to-ground thermal resistance. When the ground heat exchanger consists of coaxial pipes, a uniform heat flux along the boreholes is representative for large fluid flow rates, whereas a uniform wall temperature is more suitable for low flow rates. The distinction is given by the smallest effective resistance value calculated for both cases With U-pipes installations, a uniform wall temperature is appropriate for the whole range of flow rates. Finally, the local solutions should be able to take into consideration a connection in series of the boreholes, as well as a vertical division of the store volume.

5. DEVELOPMENT OF TRNSYS SYSTEMS

The developed TRNSYS systems are based on the two system designs described in chapter 3 (system with or without water buffer tank). Comparisons with detailed programmes (see chapter 3 for a description of the programmes) are performed for a typical summer month (June), and provide a mutual validation of the TRNSYS systems and the detailed programmes for this particular case. Some modifications have to be made to the TRNSYS systems, so that they can reproduce the thermal performances of a real system. TRNSYS 13.1 [1] is used for the development of the TRNSYS systems. In addition to the standard components, the following special components are used:

- DST component [2]; it simulates a seasonal duct store in the ground (see chapter 3). A description of the model is given by Hellström [3].
- XST component [4]; it simulates a seasonal water store in or on the ground. The component is based on the SST model [5]. The XST component can support up to 4 flow loops whose inlet and outlet pipes to or from the store can be connected at user-specified levels.
- Matched Flow Collector (MFC) component [6]; it simulates a collector array with a second order collector equation that include heat capacitive effects.

The use of the MFC or standard collector component (with or without heat capacity), together with the two basic system designs, leads to 4 TRNSYS systems.

5.1 System Design without Buffer

The layout of the system design is given in Fig. 5.1. (See chapter 3 for the description and operation of the system.) In Fig. 5.2, the system is shown according to PRESIM [7], a user-friendly pre-processor, devised to develop representations of real systems by assembling components in an interactive graphical mode. PRESIM produces a TRNSYS deck that can be computed by TRNSYS. The components designed to read and process weather data are not shown in Fig. 5.2.

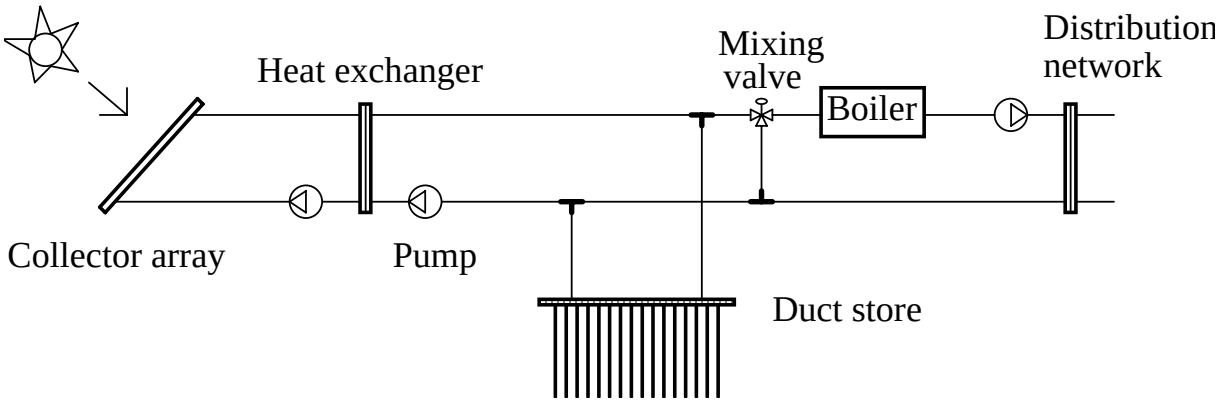

Fig. 5.1 Design of the system without buffer tank.

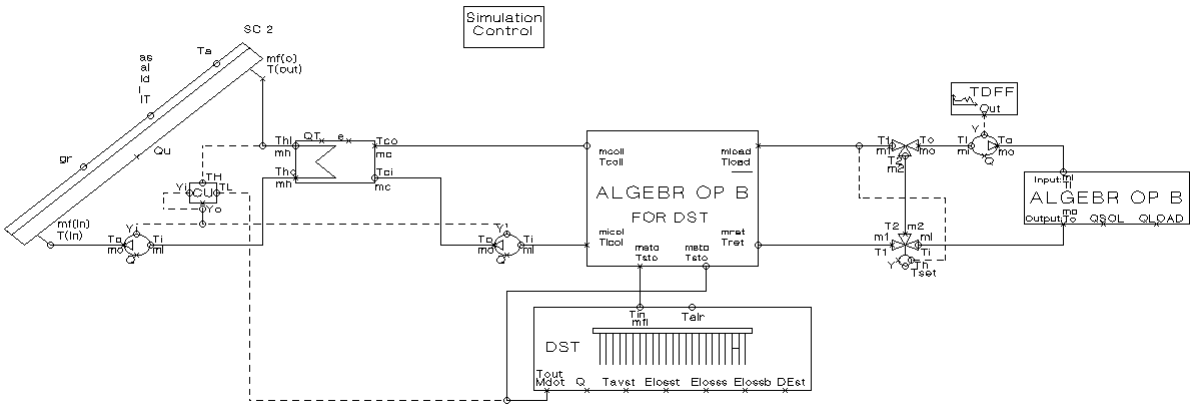

Fig. 5.2 PRESIM representation of the system without buffer tank.

5.1.1 Algebraic Operator for DST

The collector array is connected to the duct store (via a heat exchanger), but a direct connection to the heat load is also provided by the system layout (see Fig. 5.1). In consequence, the fluid flowing to or from the duct store may circulate in both directions, depending on the operation mode of the system (loading or unloading the duct store). In a TRNSYS system, the fluid can only move in one direction (an input variable can not be an output variable). This difficulty has been overcome with the use of an "Algebraic Operator" component. In order to achieve the required task, 6 input variables are computed to generate 6 output variables, with the help of 102 parameters. The 6 input variables are:

- $m_{from\ coll}$, $T_{from\ coll}$: flow rate and temperature of the heat carrier fluid from the collector array (on the store side of the solar heat exchanger);
- $m_{from\ load}$, $T_{from\ load}$: flow rate and temperature of the heat carrier fluid from the load subsystem;
- $m_{from\ duct}$, $T_{from\ duct}$: flow rate and temperature of the heat carrier fluid from the duct store.

The 6 outputs are:

- $m_{to\ coll}$, $T_{to\ coll}$: flow rate and temperature of the heat carrier fluid toward the collector array (on the store side of the solar heat exchanger);
- $m_{to\ load}$, $T_{to\ load}$: flow rate and temperature of the heat carrier fluid toward the load subsystem;
- $m_{to\ duct}$, $T_{to\ duct}$: flow rate and temperature of the heat carrier fluid toward the duct store.

The circulation of the fluid in closed loops requires that:

- the flow rates to and from the collectors are equal;
- the flow rates to and from the duct store are equal;
- the flow rates to and from the load subsystem are equal.

The 6 outputs are computed by the 102 parameters that perform the following operations with the 6 inputs:

$$m_{to\ duct} = abs(m_{from\ coll} - m_{from\ load}) \quad (5.1)$$

$$T_{to\ duct} = T_{from\ coll} \quad IF \quad m_{from\ coll} > m_{from\ load} \quad (5.2a)$$
$$T_{to\ duct} = T_{from\ load} \quad IF \quad m_{from\ coll} \leq m_{from\ load} \quad (5.2b)$$

$$m_{to\ load} = m_{from\ load} \quad (5.3)$$

$$T_{to\ load} = T_{from\ coll} \quad IF \quad m_{from\ coll} > m_{from\ load} \quad (5.4a)$$
$$T_{to\ load} = (T_{from\ coll} \cdot m_{from\ coll} + T_{from\ duct} \cdot m_{from\ duct})/(m_{from\ coll} + m_{from\ duct})$$
$$IF \quad (m_{from\ coll} \leq m_{from\ load}) \ AND \ (m_{from\ coll} + m_{from\ duct} > 0) \quad (5.4b)$$
$$T_{to\ load} = T_{from\ duct} \quad IF \quad (m_{from\ coll} \leq m_{from\ load}) \ AND \ (m_{from\ coll} + m_{from\ duct} \leq 0) \quad (5.4c)$$

$$m_{to\ coll} = m_{from\ coll} \quad (5.5)$$

$$T_{to\ coll} = T_{from\ load} \quad IF \quad m_{from\ coll} < m_{from\ load} \quad (5.6a)$$
$$T_{to\ coll} = (T_{from\ load} \cdot m_{from\ load} + T_{from\ duct} \cdot m_{from\ duct})/(m_{from\ load} + m_{from\ duct})$$
$$IF \quad (m_{from\ coll} \geq m_{from\ load}) \ AND \ (m_{from\ load} + m_{from\ duct} > 0) \quad (5.6b)$$
$$T_{to\ coll} = T_{from\ duct} \quad IF \quad (m_{from\ coll} \geq m_{from\ load}) \ AND \ (m_{from\ load} + m_{from\ duct} \leq 0) \quad (5.6c)$$

The inlet flow rate and fluid temperature to the duct store, provided by the "Algebraic Operator", corresponds physically to two different pipes. When the store is loaded ($m_{from\ coll} > m_{from\ load}$) after a period of discharge ($m_{from\ coll} < m_{from\ load}$), the circulation of the fluid is reversed. The inlet pipe becomes the outlet pipe and vice versa. This is automatically performed inside the DST component, when an injection period follows an extraction period (or vice versa).

5.1.2 System Control

The system control is ensured by a solar controller for the operation of the collector array, a forcing function to simulate the variable flow rate in the load subsystem and a mixing valve. The heat load is reduced to the domestic hot water requirements (heat losses included) with a pre-defined daily profile given hour by hour (see chapter 3). The mixing valve ensures that the forward temperature to the load subsystem does not exceed its prescribed value (55°C). It

also permits the disconnection of the solar collectors and the duct store from the rest of the system if the forward temperature is lower than the return temperature.

Knowing the forward and return load temperatures (55°C and 30°C), together with the heat load demand, the flow rate of the load pump is set hour by hour by the means of a forcing function. The heat supplied by the boiler is calculated by the second "Algebraic Operator" component, knowing the temperature difference between the required load temperature (55°C) and the actual forward temperature in the load subsystem.

The solar controller controls the two pumps on both sides of the solar heat exchanger. The control command (ON or OFF) depends on the difference of two temperatures, an upper and lower one. The difference is compared with two prescribed temperature differences, or dead-band temperature differences; one to start the pumps and one to stop them. The dead-band temperature differences are chosen so that a hysteresis effect is provided. A natural choice for the upper and lower temperatures is the outlet fluid temperature of the collector array and the inlet fluid temperature in the solar heat exchanger (on its secondary side, before the pump).

The choice of the lower temperature provokes instability problems. When the collector array is off, the lower temperature is given by the fluid temperature from the load. There are hours where the collector array can be turned on, but in this case, the lower temperature is higher due to the outlet temperature from the duct store, and the collector array has to be turned off. The lower temperature drops back to the load-fluid temperature and the problem recommences. After a given number of oscillations, the control command is blocked at its last value. It can be blocked in the wrong state, either dissipating heat through the collector array or not collecting available solar heat as a result. These situations usually occur during the summer, when the temperature difference between the duct store and the return fluid from the load subsystem is large. These effects are small, provided that the hysteresis effect of the controller is sufficiently large and the collector heat capacity is not accounted for in the simulation. This is not the case if a collector component with heat capacity is used. Some simulations with a value of 20 kJ/m^2K showed irrelevant results. (The collected energy was sensitive to the number of oscillations permitted (up to 10% difference for a summer month), or the dissipated heat through the collector array could attain 20% of the collected energy during a summer month!).

A better choice for the lower temperature of the solar controller is the outlet temperature returned by the DST component. During the summer, the solar array essentially feeds the duct store. The heat delivered directly to the load is marginal. In that respect, the outlet fluid temperature of the duct store is more appropriate for the operation of the collector array. This choice has suppressed all of the problems relating to instability. The control command of the solar controller was not blocked as no heat was dissipated in the collector array (with or without heat capacity taken into account in the collector array). When the heat capacity of the collector array is not accounted for, both choices of the contoller's lower temperature give similar results. The collected energy, using the same dead-band temperature differences, matches within 1% (see next section).

5.1.3 TRNSYS System with the Standard Collector Component (System without Buffer Tank)

Parameters defining each component are set so that the TRNSYS system corresponds to the reference system defined in chapter 3. In order to permit comparisons of the systems' performances, the duct store in the TRNSYS system is perfectly insulated. In the detailed programme described in chapter 3, the heat capacitive effects of the fluid in the ground heat

exchanger are not taken into account, the thermal borehole resistance is set to a constant value (0.1 K/(W/m)) and the vertical division of the store volume is reduced to 1 cell.

The collector array is characterised by an average transmittance-absorptance product of 0.75 and an overall loss coefficient of 3.5 W/m^{2}K (both values take into account the collector efficiency factor F'). In the standard collector component (type 1), these values have to be corrected by F_R, the collector heat removal factor corresponding to the flow rate in test conditions. With the flow rate of the reference system (0.007 kg/m^{2}sec), the collector parameters become respectively 0.707 and 3.3 W/m^{2}K.

The thermal performances of the system are simulated for the month of June 1988, with hourly weather values measured at Nykvarn, a northern location at 59.2° latitude (see chapter 3 for additional details). Monthly collected energies simulated for different values of the dead-band temperature differences of the solar controller in TRNSYS are shown in table 5.1. The lower temperature of the controller is chosen as the outlet temperature returned by the store component.

	Collected energy during the month of June		Dead-band temperature differences of the solar controller (TRNSYS system)
Detailed programme	1'871 MWh		-
TRNSYS system	1'870 MWh	-0%	0 - 0 K
	1'870 MWh	-0%	0 - 2 K
	1'868 MWh	-0.2%	0 - 5 K
	1'860 MWh	-0.6%	0 - 10 K
	1'853 MWh	-1.0%	0 - 14 K
	1'841 MWh	-1.6%	2 - 2 K
	1'840 MWh	-1.7%	2 - 5 K
	1'835 MWh	-1.9%	2 - 14 K

Table 5.1 Comparison of the collected energy computed by the detailed programme and the TRNSYS programme. Simulations performed with TRNSYS are shown for different values of the dead-band temperature differences of the solar controller. (The second value is the temperature difference needed to turn the collector array on and the first to turn it off.) Simulations are performed on the reference system and a borehole thermal resistance set to 0.1 K/(W/m).

In Fig. 5.3 and 5.4, hourly values of the collected energy are compared. The values computed by TRNSYS are plotted against the values computed by the detailed programme. In the TRNSYS system, the dead-band temperature differences of the solar controller are set to 2 and 14 K. The TRNSYS calculations differ from Fig. 5.3 and 5.4 only by the choice of the controller's lower temperature. In Fig. 5.3, the lower temperature is chosen as the inlet fluid temperature in the solar heat exchanger (on the store side), and in Fig. 5.4 as the outlet fluid temperature returned by the store component. With the second choice, the monthly collected energy is slightly decreased by 0.8%. But with the first choice, the control command of the solar controller is sometimes blocked in the wrong state, and can result in heat dissipated through the collector array.

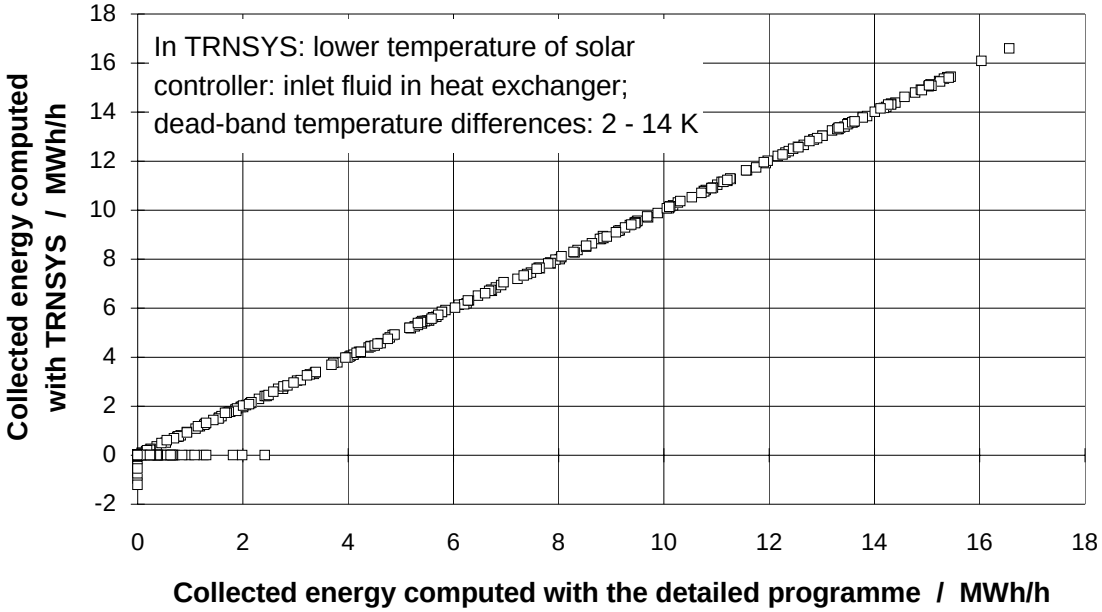

Fig. 5.3 Comparison of the collected energy in hourly values. The values computed by TRNSYS are plotted against the values computed by the detailed programme. In the TRNSYS deck, the lower temperature of the solar controller is the inlet fluid temperature in the solar heat exchanger (on the store side).

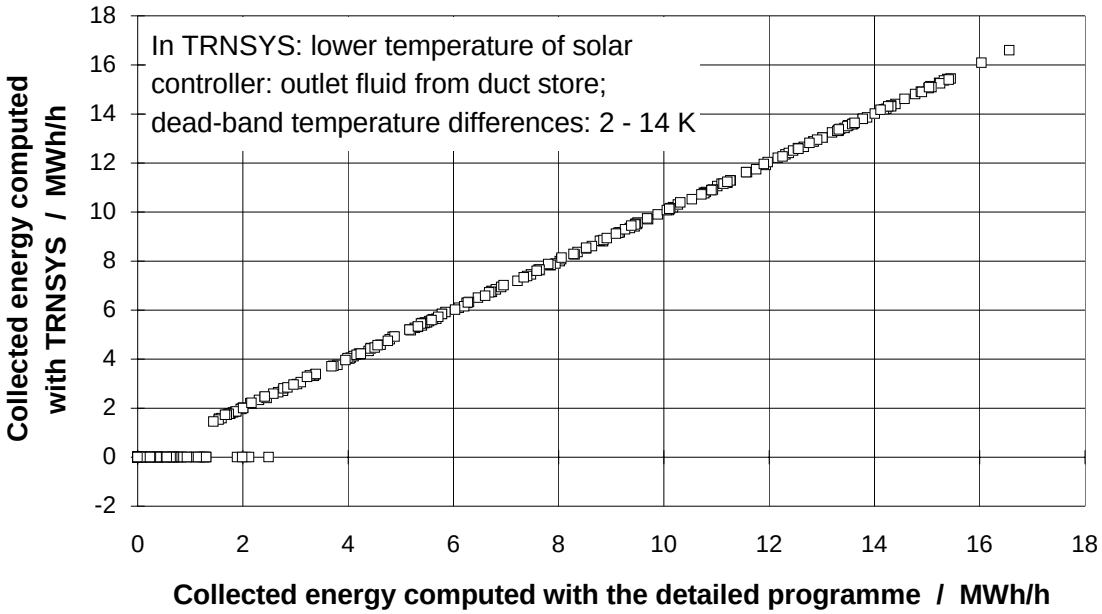

Fig. 5.4 Comparison of the collected energy in hourly values. The values computed by TRNSYS are plotted against the values computed by the detailed programme. In the TRNSYS deck, the lower temperature of the solar controller is the outlet fluid temperature returned by the store component (DST).

The monthly collected energy computed by TRNSYS, in comparison to that computed with the detailed programme, is 1.2 % lower in Fig. 5.3 and 1.9 % lower in Fig. 5.4. If the values affected by a wrong control command are eliminated, the collected energy computed by TRNSYS is 0.2% larger than that computed by the detailed programme. For all other

computations, the controller's lower temperature is chosen as the outlet fluid temperature returned by the store component.

5.1.4 TRNSYS System with the MFC Collector component (System without Buffer Tank)

The heat capacitive effects of the collector array are accounted for by the MFC component. A new TRNSYS system is built by simply exchanging the standard collector component with the MFC component. In this component, the average transmittance-absorptance product and the overall loss coefficient correspond to respectively 0.75 and 3.5 W/m^{2}K (local values). The quadratic term for the loss factor is not used and is set to zero.

The result of a simulation should not be significantly sensitive to the simulation time-step. This was the case with a simulation time-step of one hour in the previous computations. If the heat capacity of the collector array is taken into account, the simulation time-step has to be decreased. In table 5.2, the monthly collected energy is calculated for different values of simulation time-step and collector heat capacity. Simulations are performed with the reference system (borehole thermal resistance set to 0.1 K/(W/m) and dead-band temperature differences of the solar controller set to 0 - 14 K). Hourly weather values measured during the month of June 1988 at Nykvarn were used.

Collected energy MWh (month of June)		Simulation time-step: 1 hour	15 minutes	6 minutes	3 minutes
Collector heat capacity:	1 kJ/m^{2}K	1'846 (99.9%)	1'847 (100%)	1'848 (100%)	1'848 (100%)
	10 kJ/m^{2}K	1'797 (99.1%)	1'803 (99.4%)	1'805 (99.6%)	1'813 (100%)
	20 kJ/m^{2}K	1'716 (97.4%)	1'739 (98.7%)	1'758 (99.8%)	1'762 (100%)
	30 kJ/m^{2}K	1'648 (96.9%)	1'671 (98.3%)	1'696 (99.8%)	1'700 (100%)

Table 5.2 Simulated monthly collected energy using the reference system and different values of simulation time-step and collector heat capacity. The percentage refers to the corresponding collected energy calculated with the smaller simulation time-step.

In Fig. 5.5, a comparison of the monthly collected energy with the detailed programme is made. The one-node collector model with heat capacity is implemented in the detailed programme (see chapter 3). In the TRNSYS system, the dead-band temperature differences are set to 0 - 14 K and the simulation time-step is set to 3 minutes.

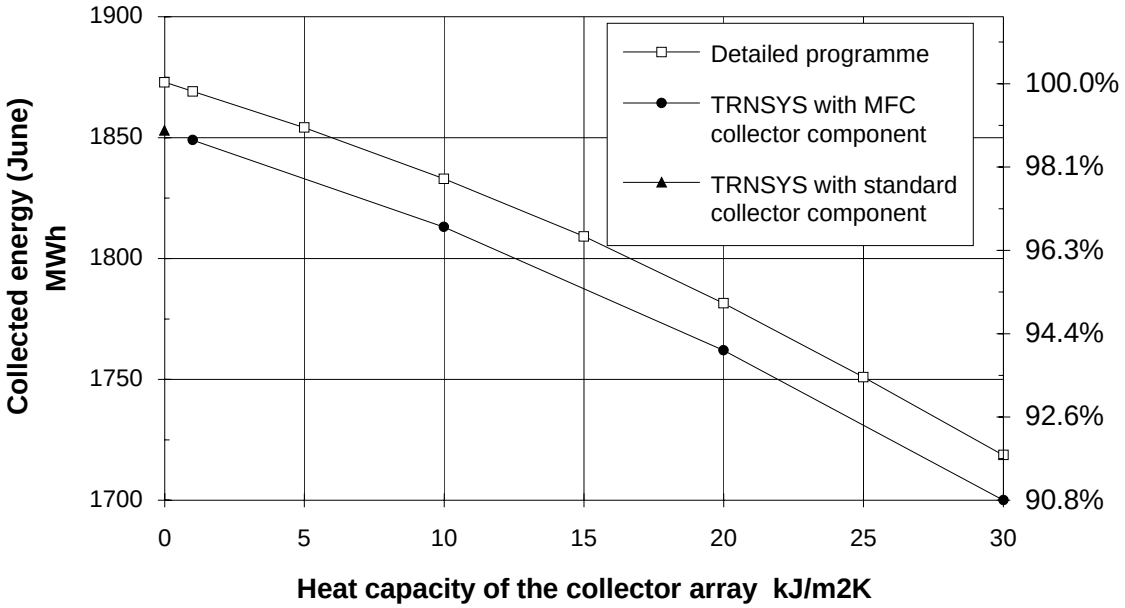

Fig. 5.5 Monthly collected energy calculated with TRNSYS and the detailed programme for different values of collector heat capacity. The percentage refers to the value of the collected energy simulated without collector heat capacity and with the detailed programme.

The differences between TRNSYS and the detailed programme are mainly due to the system control in TRNSYS (dead-band temperature differences). Apart from this, the curves have almost the same shape, showing that the heat capacitive effects on the monthly collected energy is quite similar in both cases. Furthermore, the correspondence between the TRNSYS simulation using the MFC collector component and the standard collector model is quite satisfactory when the collector heat capacity is negligible.

5.2 System Design with Buffer Tank

The layout of the system design is given in Fig. 5.6 (see chapter 3 for the description and operation of the system). In Fig. 5.7, the system is shown according to PRESIM. The components designed to read and process weather data are not shown in Fig. 5.7. In the TRNSYS system, 4 flow loops are connected to the short term buffer tank (modelled with the XST component). Two flow loops are used to load or unload the duct store, one for the collector array and one for the load subsystem.

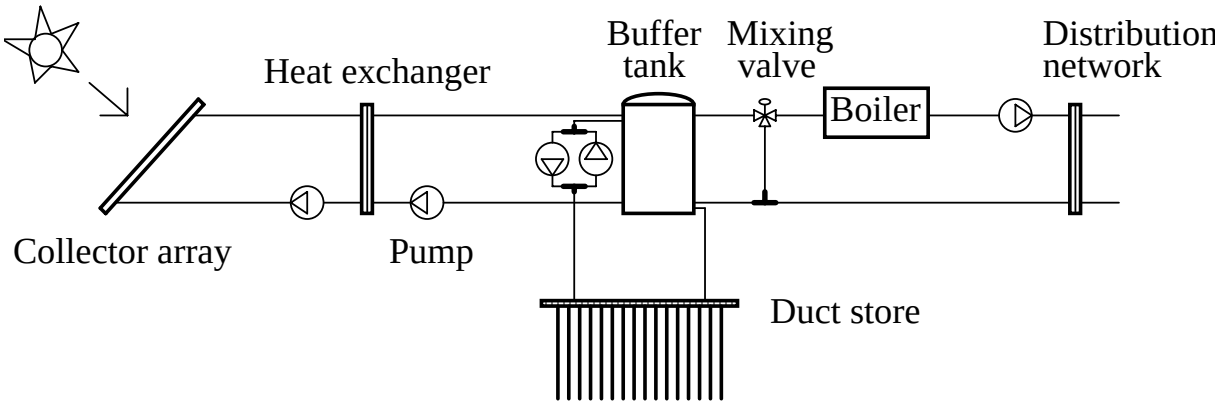

Fig. 5.6 Design of the system with buffer tank.

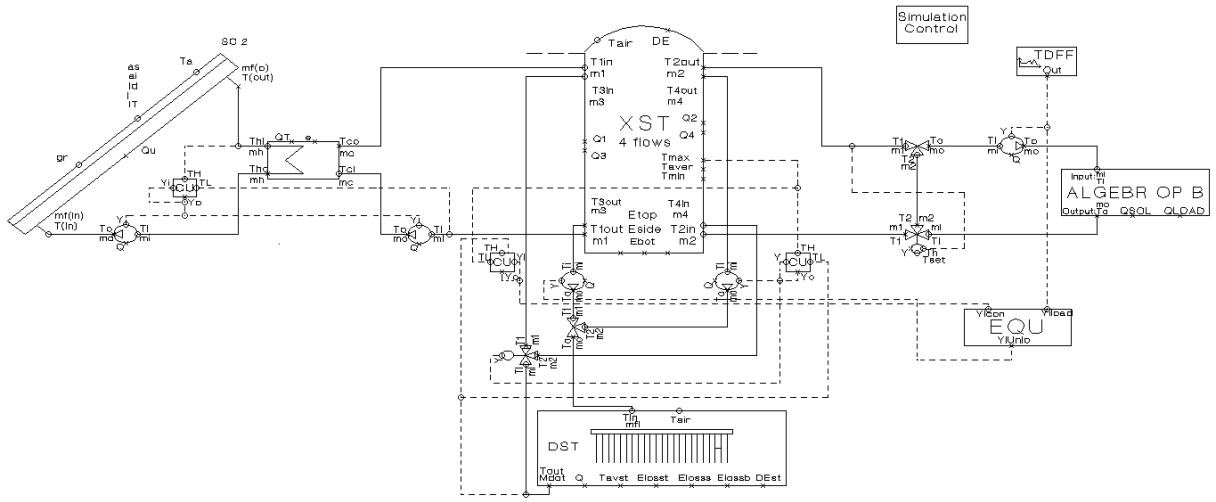

Fig. 5.7 PRESIM representation of the system with buffer tank.

5.2.1 System control

The collector array is controlled in the same way as with the system design without buffer tank, but the controller's lower temperature is chosen as the outlet fluid temperature at the bottom of the buffer tank. The load subsystem is also controlled as in the system design without buffer. The duct store is controlled according to the basic strategy defined in chapter 3. The two pumps are controlled by two "ON/OFF" controllers, each having two dead-band temperature differences.

When the duct store is loaded by the buffer, water is taken at the top of the buffer, pushed through the ground heat exchanger and re-injected at the bottom of the buffer. In the basic strategy, the loading flow rate is constant, set to half of the nominal flow rate in the collector array. The loading pump is controlled by the loading controller. The upper and lower temperatures of the loading controller are chosen as the maximum fluid temperature in the buffer tank and the outlet fluid temperature from the duct store.

When the duct store is unloaded into the buffer, the fluid circulates in the opposite direction. Water is taken out at the bottom of the buffer, pushed through the ground heat exchanger and re-injected at the top of the buffer. In the basic strategy, the unloading flow

rate is set to the actual flow rate in the flow loop of the load subsystem. The unloading pump is controlled by the unloading controller. The upper and lower temperatures of the unloading controller are chosen as the outlet fluid temperature from the duct store and the maximum fluid temperature in the buffer tank. In order to achieve a variable flow rate, the control signal to the unloading pump is obtained by the product of the signal of the unloading controller (1 or 0) and the forcing function defined to operate the pump in the load subsystem.

In the TRNSYS system, a flow diverter is placed on the outlet pipe of the duct store component. It is controlled by the load controller which ensures that the fluid returns at the correct level in the buffer tank.

5.2.2 TRNSYS System with the Standard Collector Component (System with Buffer Tank)

Parameter values of the TRNSYS system are set so that the system corresponds to the reference system with a buffer tank of 5'000 m^3 (see chapter 3 for additional details). In order to permit comparison with the detailed programme (which simulates the reference system with buffer tank), the duct store and the buffer tank in the TRNSYS system are perfectly insulated. In the detailed programme, the heat capacitive effects of the fluid in the ground heat exchanger are not taken into account, the thermal borehole resistance is set to a constant value (0.1 K/(W/m)) and the vertical partition of the store volume is reduced to 1 cell.

The thermal performances of the system are simulated for the month of June 1988, with hourly weather values measured at Nykvarn (northern location at 59.2 latitude; see chapter 3). In table 5.3, the thermal performances, simulated by TRNSYS and the detailed programme, are presented for comparison. In the TRNSYS system, the dead-band temperature differences are set to 0 - 5 K for the solar controller and 0 - 0.1 K for the loading and unloading controller. Furthermore, the number of segments in the buffer tank (see chapter 3) had to be limited to 3. The number of segments is limited by the simulation time-step (1 hour in this TRNSYS system), the largest flow rate through the buffer and its volume. The volume of fluid moved during one time-step must always be smaller than the volume of a segment. One possibility for increasing the number of segments is to decrease the length of the simulation time-step. This action is compatible with the use of a collector component with a heat capacity. The time required to perform one simulation will increase. Assuming that computers become faster, this is not a problem.

Month of June	Detailed programme (25 segments in the buffer)	Detailed programme (3 segments in the buffer)	TRNSYS (3 segments in the buffer)
Collected energy	2'230 MWh	2'199 MWh	2'205 MWh
Stored energy in duct store	1'814 MWh	1'777 MWh	1'783 MWh
Stored energy in buffer tank	111 MWh	117 MWh	117 MWh
Energy delivered to the consumer	305 MWh	305 MWh	305 MWh
Maximum fluid temperature in the ground heat exchanger	88.0 °C	86.8 °C	86.6 °C

Table 5.3 Monthly thermal performances simulated with the detailed programme and TRNSYS. The reference system with a buffer volume of 5'000 m^3 is used to perform the simulations (month of June).

5.2.3 TRNSYS System with the MFC Collector Component (System with Buffer)

This TRNSYS system is created by exchanging the standard collector component with the MFC collector component (having compatible parameters). The simulation time-step is set at 15 minutes, and permits an increase of the number of segments in the buffer to 14. The dead-band temperature differences are left at the values given in the TRNSYS system with the standard collector component. Simulations are performed under the same conditions as those given in the previous section, and with a collector heat capacity of 20 kJ/m^2K in the TRNSYS and detailed programmes. The thermal performances simulated with both programmes are presented in table 5.4 for comparison.

Month of June	Detailed programme (25 segments in the buffer)	TRNSYS (14 segments in the buffer)
Collected energy	2'147 MWh	2'131 MWh
Stored energy in duct store	1'737 MWh	1'719 MWh
Stored energy in buffer tank	106 MWh	108 MWh
Energy delivered to the consumer	304 MWh	304 MWh
Maximum fluid temperature in the ground heat exchanger	86.8 °C	86.3 °C

Table 5.4 Monthly thermal performances simulated with the detailed programme and TRNSYS. The simulations are performed using the reference system, a buffer tank of 5'000 m^3 and a collector heat capacity of 20 kJ/m^2K.

5.3 Simulation Examples during the Life-Time of a System

With the two basic system designs (with or without short term buffer tank), simulations during the life-time of a system can be performed. In this section, simulations are performed over 20 years using the reference system, in order to give examples of system performance over a long period of time (including transient effects). They also provide an example of the heat capacitive effects of the collector array. In one particular case, they show how the system performances are improved when a 5'000 m^3 buffer tank is inserted in the reference system.

To achieve these tasks, a year of hourly weather data is used, the heat load is completed with the space heating demand and some system parameters are modified to take into account various effects (incidence angle modifier, store heat losses, warming of the surrounding ground, etc.).

5.3.1 Weather Data

The weather data was measured in 1991 at Göteborg (Sweden, northern location, latitude 57.8°, longitude 12° East). Different variables were recorded on an hourly basis (outdoor temperature, total horizontal radiation per unit area, incident beam radiation per unit area, etc.). The mean annual temperature corresponded to 9 °C, with extreme daily values at 24 °C and -7 °C. The global horizontal insulation reached 950 kWh/m^2year. The total incident radiation in the collector plane (facing south and tilted to 30° relative to horizontal) is calculated at 1'120 kWh/m^2year (TRNSYS calculation using the Perez model [8] to transpose the measured radiation onto the collector plane). The weather data set is repeated 20 times.

5.3.2 Heat Load

The same procedure as that given in chapter 7 is followed. The heat load is defined by assuming that the domestic hot water requirement represents 30% of the total heat requirement. In respect to the domestic hot water requirement defined in the reference system (daily values are assumed to be constant during the year), the space heating heat demand is defined as follows:

$$\text{If } T_{out} < 13\ °C \quad \text{Then} \quad P_{sh}\ [kW] = 100\ [kW/K] \cdot (19 - T_{out})\ [K] \qquad (5.1a)$$

$$\text{Else} \quad P_{sh} = 0 \qquad (5.1b)$$

T_{out}: hourly outdoor temperature;
P_{sh}: hourly space heating heat demand.

The total annual heat demand, calculated with the weather data measured in 1991 in Göteborg, corresponds to 12'600 MWh/year (space heating: 8'700 MWh/year and domestic hot water: 3'900 MWh/year).

The forward and return fluid temperatures in the load subsystem depend on the outdoor temperature according to the graph in Fig. 5.8.

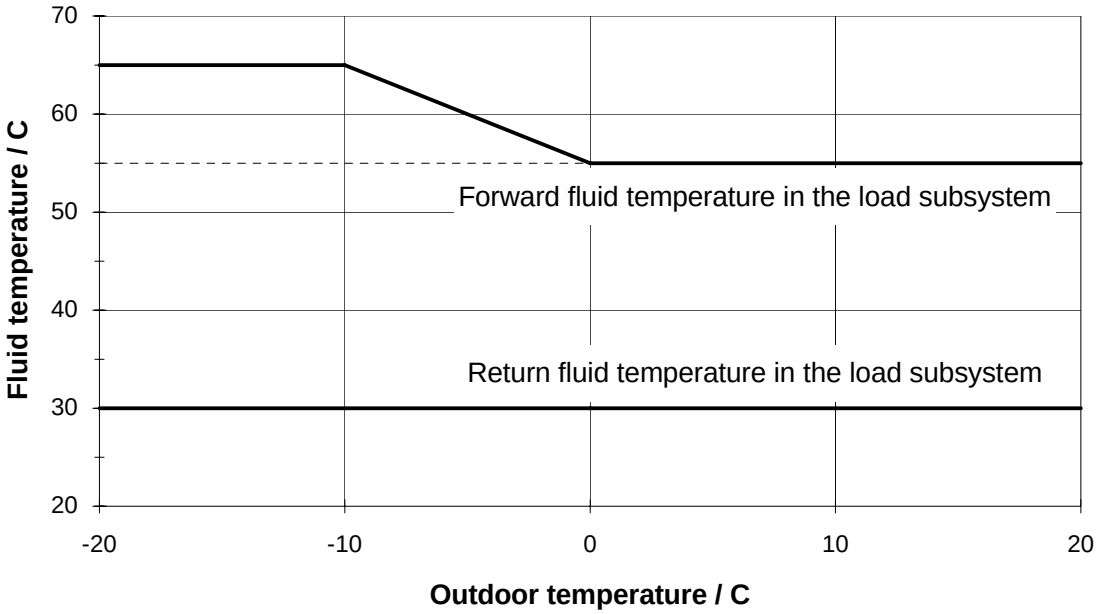

Fig. 5.8 The forward and return fluid temperatures in the load subsystem are specified and depend on the outdoor temperature.

The mixing valve in the load subsystem ensures that the forward temperature does not exceed its prescribed value. This latter is now dependant on the outdoor temperature. The flow rate in the load subsystem is fixed once the total heat demand and forward and return fluid temperatures are known. This is achieved by various equations and an algebraic operator in the TRNSYS deck.

5.3.3 System parameters

The parameter values of the system are set to those given in the reference system defined in chapter 3. Nevertheless, some parameters have to be modified, so that different effects are taken into account (incidence angle modifier, store heat losses, warming of the surrounding ground, etc.). All the parameters are listed in table 5.5.

SOLAR COLLECTORS:	
Location:	latitude: 59.2° North longitude: 17.4° East
Orientation:	azimuth: 0° (South facing) tilt angle (with respect to horizontal plane): 38°
Area:	35'000 m^2
Specific flow rate:	0.007 kg/sec /m^2 of collector area (loading flow rate)
Heat carrier fluid:	water
Average transmittance-absorptance product:	0.75 (-) (corrected by the collector efficiency factor F')
Overall loss coefficient:	3.5 W/m^2K (corrected by the collector efficiency factor F')
Collector heat capacity:	10 kJ/m^2K
Incidence angle modifier:	0.1 (parameter bo in 1 - bo (1/cosθ - 1))
Solar controller:	dead-band temperature differences:2 - 14 K

Table 5.5a Parameters defining the TRNSYS systems based on the reference system.

SOLAR HEAT EXCHANGER (counter flow)	
UA_value:	120 W/K /m^2 of collector area
Specific flow rate secondary side:	0.007 kg/sec /m^2 of collector area (loading flow rate)
DUCT HEAT STORAGE	
Volume:	350'000 m^3
Depth:	125 m
Number of boreholes:	359
Distance between ground surface and upper side:	1m
Insulation:	thermal conductivity: 0.05 W/mK
	thickness: 0.2 m
	location: on top (the horizontal extension from the edge of the store equals 10% of its depth)
Ground heat exchanger:	
	heat carrier fluid: water
	open annular duct, hexagonal pattern
	spacing between boreholes: 3 m
	borehole diameter: 0.115 m
	inner pipe: outer diameter: 0.063 m
	thickness wall: 0.0058 m
	thermal conductivity of pipe material: 0.2 W/mK
	borehole thermal resistance: 0.01 K/(W/m)
Rock:	thermal conductivity: 3.5 W/mK
	volumetric heat capacity: 2.2 MJ/m^3K
Initial store and ground temperature:	10 °C
SHORT-TERM BUFFER TANK (if present in the system)	
Volume:	5'000 m^3
Vertical extension:	10 m
	number of segments: 14
Connecting pipes:	top and bottom of the buffer
Insulation:	thermal conductivity: 0.05 W/mK
	thickness: 1m
	location: uniformly placed on buffer envelope
Load controller (duct store):	dead-band temperature differences: 1 - 5 K
Unload controller (duct store):	dead-band temperature differences: 1 - 5 K
HEAT LOAD	
Domestic hot water (including heat losses):	3'900 MWh/year (30%)
Space heating requirement:	8'700 MWh/year (70%)
Annual heat load:	12'600 MWh/year (100%)
Forward temperature:	55 °C
Return temperature:	30 °C

Table 5.5b Parameters defining the TRNSYS systems based on the reference system.

5.3.4 Simulation results

Simulations start in January. In table 5.6 and 5.7, the system performances are given year by year for each of the two systems (with and without buffer tank). Among the different variables presented in the tables, the *duct store efficiency* is defined as the ratio between the extracted and injected energy during a cycle. The *duct store fraction* indicates the proportion of the total heat demand covered by the extracted energy. One simulation (20 years) lasts about 50 minutes, using a 32-bits Fortran compiler on a personal computer PENTIUM 60 MHz.

Year	Collector array MWh/year	annual efficiency	Duct store efficiency	fraction	Solar heat MWh/year	System efficiency	Solar fraction
1	13'900	35.5%	25.5%	26.3%	4'200	10.8%	33.5%
2	11'500	29.4%	62.8%	51.8%	7'600	19.5%	60.4%
3	11'200	28.5%	73.2%	58.5%	8'500	21.6%	67.1%
4	11'100	28.2%	76.7%	60.6%	8'700	22.3%	69.1%
5	11'000	28.1%	78.6%	61.7%	8'900	22.6%	70.2%
10	10'900	27.7%	82.4%	63.9%	9'100	23.3%	72.4%
15	10'800	27.6%	83.7%	64.6%	9'200	23.5%	73.1%
20	10'800	27.6%	84.5%	65.1%	9'300	23.7%	73.5%
Total	11'100	28.2%	77.1%	61.1%	8'800	22.4%	69.5%

Table 5.6 System performances simulated with the completed reference system (without buffer tank).

Year	Collector array MWh/year	annual efficiency	Duct store efficiency	fraction	Solar heat MWh/year	System efficiency	Solar fraction
1	15'400	39.2%	13.1%	12.5%	4'800	12.1%	37.8%
2	12'900	33.0%	43.2%	25.9%	8'600	21.9%	68.1%
3	12'500	32.0%	57.6%	32.3%	9'500	24.2%	75.4%
4	12'400	31.6%	62.9%	34.4%	9'800	25.0%	77.8%
5	12'300	31.4%	65.9%	35.6%	10'000	25.4%	79.0%
10	12'200	31.0%	71.6%	37.8%	10'200	26.1%	81.3%
15	12'100	30.9%	73.7%	38.5%	10'300	26.4%	82.1%
20	12'100	30.9%	74.9%	38.8%	10'400	26.5%	82.3%
Total	12'400	31.6%	64.2%	35.6%	9'800	25.1%	78.1%

Table 5.7 System performances simulated with a buffer tank in the completed reference system.

Monthly heat balances and temperature levels associated with some heat quantities are shown in figures 5.9 and 5.10 for the 20th year of operation.

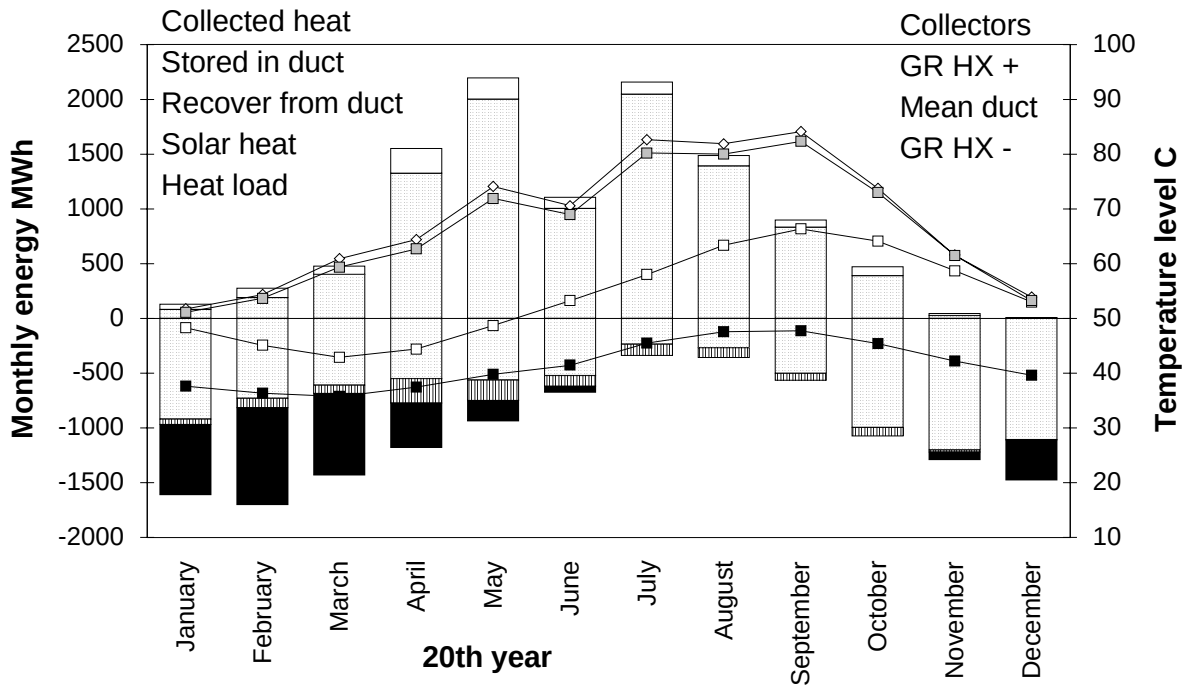

Fig. 5.9 Monthly heat balance simulated for the system without buffer tank. The positive energy columns represent the collected heat and the negative columns the heat load. The difference between the collected heat and the stored heat in the duct store, is the solar heat that directly feeds the heat load. The total solar heat comprises this contribution and the recovered energy from the duct store. The temperature levels in the collector array, the ground heat exchanger during heat injection, the duct store, as well as the ground heat exchanger during heat abstraction, are shown respectively from top to bottom.

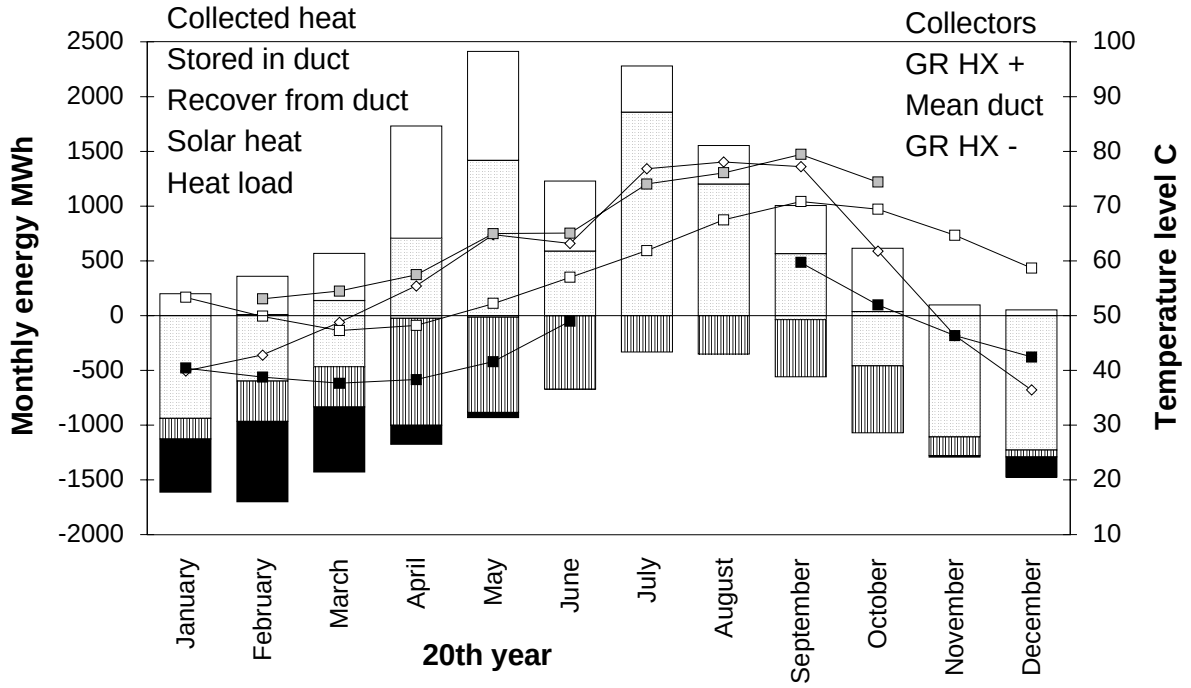

Fig. 5.10 Monthly heat balance simulated for the system with buffer tank. Same legend as for fig. 5.9, but this time the difference between the collected heat and the stored heat in the duct store also includes the short-term heat storages in the buffer tank. The same temperature levels as in figure 5.9 are shown with the same labels.

The mean temperature level relative to a heat quantity is defined as an average value; obtained with a multiple integration over time and heat transfer area, of the fluid temperature weighted by the instantaneous and punctual heat transfer flux [9]. A rough estimation of the mean temperature level is calculated by weighting the mean fluid temperature; set as the arithmetic mean between inlet and outlet, with the corresponding heat transfer rate.

The cost of the different subsystems is not considered in these examples. In consequence, the two systems are not optimised. The system with buffer tank would be more expensive, but the solar heat is 10% higher. Nevertheless, the simulated thermal performances of the system without buffer tank are not realistic, as the maximum fluid temperature in the ground heat exchanger sometimes reaches 100 °C. After 10 years, the mean temperature of the duct store varies between 42 and 67 °C. In this system, the ratio *store volume* over *collector area* is not particularly low (10 m^3/m^2), the spacing between the boreholes is not especially large for rock (3m) and the borehole thermal resistance is extremely low (0.01 K/(W/m)). In order to decrease the maximum fluid temperature in the ground heat exchanger, the spacing between the boreholes can be reduced, resulting in more boreholes to drill and equip, and thus a higher cost.

The operation of the system with buffer tank is more realistic, as the maximum fluid temperature in the ground heat exchanger remains below 90 °C. After 10 years, the mean temperature of the duct store varies between 46 and 71 °C. The temperature difference between the maximum and minimum values is the same in both simulated systems. Nevertheless, the duct store fraction is much lower in the system with buffer tank (36% compared to 61%), although the solar fraction is higher (78% compared to 70%). This illustrates how a system with buffer tank behaves. The duct store is mainly used to cover the seasonal mismatch between the heat supply and the heat demand, whereas the short term mismatches are essentially covered by the buffer tank. Short-term storage in the duct store should be avoided, as it results in large quality losses of the stored energy. In fig. 5.9, heat is injected at 70-80 °C in the duct store, and recovered at 40-50 °C during the summer.

Simulations with the system without buffer tank are performed with different values of collector heat capacity. In Fig. 5.11, an example of the heat capacitive effects on the monthly collected energy is shown. The collector array is supposed to be characterised by a heat capacity of 20 kJ/m^2K. When accounted for over an operation time of 20 years, the global effect is a 6% reduction of the collected energy. The decrease of the collected energy is mainly due to the heating of the collector array. The effect is larger in winter, when usable solar gains are small.

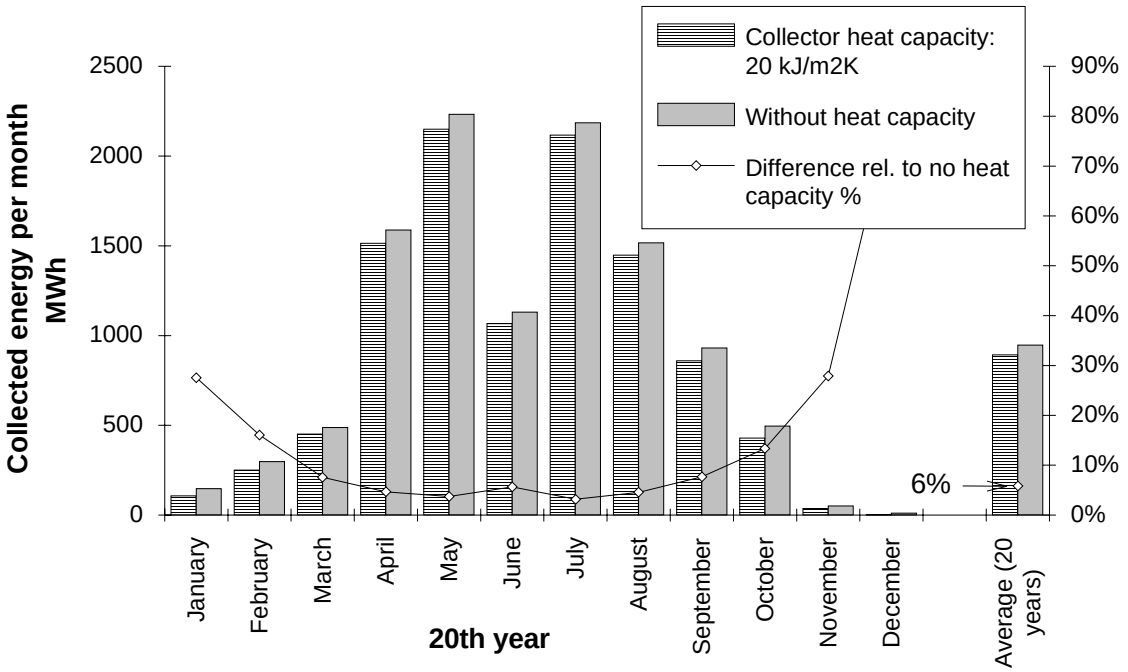

Fig. 5.11 Example of the heat capacitive effects on the monthly collected energy, simulated with the completed reference system (without buffer tank).

In Fig. 5.12, the reduction of the annual collected energy is shown in relation to different values of collector heat capacity. The reduction is plotted for the first year of operation, the 20th year and the whole period of operation. The reference values are the collected energy simulated with the standard collector component (without collector heat capacity).

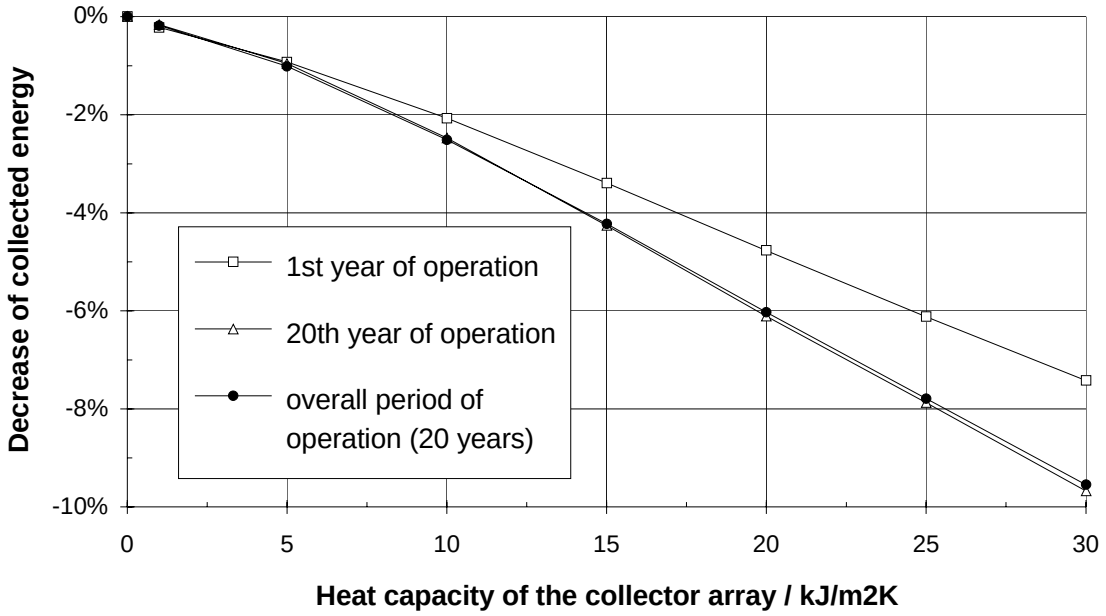

Fig. 5.12 Reduction of the annual collected energy in relation to the heat capacity that characterises the collector array. The simulations were performed with the completed reference system (without buffer tank).

The decrease of the collected energy is smaller the first year of operation, as the heat was collected at a lower temperature level. The mean temperature level is calculated at 60 °C the first year of operation, and rises up to 75 °C the 20th year. The mean value for the whole period (20 years) corresponds to 73 °C.

5.4 Necessary Improvements for the Simulation of Real Systems

The developed TRNSYS systems represent two basic designs of a CSHPSS with a duct heat store in the ground (with or without a short-term buffer tank). Nevertheless, some improvements are required before extensive simulations can be performed. A list of the main modifications is given in the following sections.

5.4.1 The Load Subsystem

The forward and return fluid temperatures have to be given on the secondary side of the load heat exchanger, so that they correspond to the forward and return fluid temperatures of the heat distribution network. (In the present developed TRNSYS systems, they are given on the primary side of the heat exchanger.) The pump flow rate on the primary side of the load heat exchanger has to be controlled so that the prescribed forward temperature in the distribution network is obtained. For this purpose, a special component has been developed and used for the simulation of the Särö solar plant [10].

A boiler component has to be added to guarantee the prescribed forward temperature on the primary side of the load heat exchanger.

5.4.2 The Collector Array

Two standard pipe components can be added to simulate the heat losses and the heat capacitive effects of the forward/return main pipes to/from the collector array. The fluid temperature from the collector array has to be limited by the maximum temperature that the rest of the system can tolerate.

5.4.3 The Duct Store Component

The flow rate and temperature of the fluid in the ground heat exchanger can significantly vary with time and from one system to another when sensitivity analysis is performed. The computation of the local process, which determines the heat rate transferred to the store, is influenced by the variations of these variables. Accurate simulations and proper sensitivity analysis should also take into account these effects.

The Fortran code of TRNDST (the DST duct store component for TRNSYS), should be completed so that the following effects are accounted for when the local process is computed:

- a radial connection of the ducts (or boreholes);
- a vertical division of the store volume;
- a heat transfer resistance between the fluid and the ground in the immediate vicinity of the duct (or borehole) that depends on the flow conditions (flow rate and temperature of the heat carrier fluid).
- axial effects due to the heat exchange between the downward and upward fluid channels. (This effect can be significant for large depths and low flow rate. See chapter 4.)

5.4.4 The Short Term Buffer Tank

The buffer tank can be simulated in the ground (XST component). One should remember that the heat losses of the buffer store do not interact with those of the duct store.

6. INFLUENCE OF PASSIVE SOLAR GAINS ON THE HEAT LOAD PROFILE

6.1 Heat Load Model with Passive Solar Gains

The following heat load model is based on the steady-state heat losses of a group of houses and a solar effective area for the collection of passive solar gains. The internal gains, due to occupancy and activities inside the housing, are assumed to be constant over the heating period.

This model is intended to generate hourly values for the heat demand of a building (or a set of buildings), which can be used by a detailed simulation programme of a solar system (TRNSYS). The hourly values calculated by the model may greatly differ from the actual values. The task of the model is to reproduce the annual heat demand and produce a conservative estimation of the heat requirement during the heating period. The peak power loads and the monthly heat demand should be reasonably close to the actual figure.

6.1.1 Parameters

Seven parameters are required for the load model; three for the heat losses, one for the internal gains and three for the passive solar gains. They are:

Tin: indoor set-point temperature [°C];
H: total specific heat losses of the housing; (transmission and ventilation losses) [kJ/hK];
Tnh: outdoor temperature heat cut-out limit.; (if the outdoor temperature exceeds this limit, then the heat requirement is assumed to be negligible) [°C];
ΔTingains: correction to the indoor set-point temperature due to the internal gains; if *Pingains* represents the heat rate generated by internal gains, the correction is given by the ratio *Pingains*/*H* [K];
Aeff: solar effective area for passive solar gains collection; this area is relative to the insolation falling on a vertical plane (preferably facing south) [m^2];
τ: time constant of the housing defined by the ratio *Ceff*/*H* [h]; *Ceff* is an effective heat capacity of the housing [kJ/K];
Tmaxin: maximum indoor temperature allowed [°C].

6.1.2 Meteorological Variables

The weather data are required on a hourly basis. Two variables are necessary:

Tout: the outdoor temperature of the air [°C];
Ivs: the global insolation on a vertical plane (facing south) [kJ/m^2h].

6.1.3 Calculated Quantities and Calculation Procedure

The following three variables are calculated. The latter two need initial values; they may be initialised at zero. (The same two variables could be reduced to 1 variable, using relation 6.2b. For the sake of clarity, this has not been done.)

Psh: heat rate required for space heating [kJ/h];
Qcapa: heat accumulated in the structure of the housing [kJ];
ΔTin: elevation of the internal temperature due to passive solar gains [K].

For each time-step the heat balance of the housing gives:

$$Psh = H \cdot [(Tin - \Delta Tingains) + \Delta Tin - Tout] - Aeff \cdot Ivs - Qcapa/\Delta t \quad (6.1)$$

Tout: outdoor temperature of the air [°C];
Δt: duration of the time-step [h].

Heat is stored in the structure of the building only if the heat rate for space heating is negative:

If (Psh < 0) AND (H > 0) AND (τ > 1 hour) Then

$$Qcapa = -Psh \cdot \Delta t \quad (6.2a)$$

$$\Delta Tin = Qcapa / (\tau \cdot H) \quad (6.2b)$$

Else

$$Qcapa = 0 \quad (6.2c)$$

$$\Delta Tin = 0 \quad (6.2d)$$

The heat demand is only considered for positive values and when the outdoor temperature is below the heat cut-out temperature limit:

$$\text{If } (Psh < 0) \text{ OR } (Tout > Tnh) \quad \text{Then} \quad Psh = 0 \quad (6.3)$$

The indoor temperature cannot exceed the maximum limit allowed:

If (Tin + ΔTin) > Tmaxin Then

$$\Delta Tin = Tmaxin - Tin \quad (6.4a)$$

$$Qcapa = (\tau \cdot H) \cdot (Tmaxin - Tin) \quad (6.4b)$$

The Degree-Day approach can be reproduced if the passive solar gains and the internal gains are not explicitely computed with Aeff and ΔTingains (Aeff = 0, τ = 0 and ΔTingains = 0). The use of the hourly rather than a daily outdoor temperature in order to determine if heating is required or not, leads to similar results. The annual heat demand does not differ by more than a few percent (with Swiss weather data used in section 6.2.3). The use of a heat cut-out temperature limit (Tnh) is a implicit way of accounting for the internal and passive solar gains. With the different cases calculated in the following sections, the values of the heat cut-out temperature limit used (Tnh = Tin - 8 K) had no influence on the annual heat demand when passive and internal gains were explicitly computed.

6.1.4 Determination of Parameters

The main parameters to be determined are the total specific heat losses H and the solar effective area Aeff of the housing. They may be assessed from measurements with the help of the *H-M diagram* [1]. If no measurements are available, the heating requirement can be assessed by the mean of a building model which performs a heat balance of the planned housing. A good example is given by the new European Standard [2] applied to an industrial building [3]. The total heat losses are explicitly calculated from the different materials forming the envelope and the air change rate of the houses. The heat losses through the ground are assumed to be small and may be expressed in relation to the outdoor temperature.

The effective area is obtained by dividing the total passive solar gains (before reducing them with a utilisation factor) by the total insolation on the south vertical plane during the heating period.

The time constant of the housing is known if the effective heat capacity of the houses can be assessed (τ = Ceff/H). This latter may be estimated following the method given in the European Standard [2]. Typically, the order of magnitude of this time constant is one day.

The other parameters are determined according to the problem under consideration.

6.1.5 Validation with Measured Data

An industrial building (68'000 m^3, 18'400 m^2) located near Geneva, Switzerland, has been analysed in great detail [3]. The heating design involves an active solar system, a gas powered heat pump (215 kW), three auxiliary furnaces (gas/oil and wood) totalling 640kW and 3'400 m^2 of double skin facades for large passive solar gains.

The thermal characteristics of the building were established for two consecutive winters with the help of the European Standard. They differ from the first winter to the second, as the state of the double skin facade was not the same (the construction was still in progress). The average indoor temperature and the load model have been determined, excepting the maximum allowed indoor temperature and the "no heating" outdoor temperature. They are set to 25 °C and 15 °C respectively; (they have no influence on the results in this case). The heat demand, also measured, is calculated with the help of the load model and the measured hourly weather data (see table 6.1).

Industrial building Marcinhès (68'000 m^3, 18'400 m^2)		
Winter	1990-1991	1991-1992
Total specific heat losses H.	18.1 kW/K	19.3 kW/K
Solar effective area Aeff:	740 m^2	650 m^2
Time constant τ:	$\approx$ 130 h	$\approx$ 130 h
Indoor temperature Tin:	17.8 °C	16.8 °C
Correction due to internal gains ΔTingains:	1.8 K	1.4 K
No heating temperature limit Tnh:	15 °C	15 °C
Maximum allowed indoor temperature Tmaxin:	25 °C	25 °C
Calculated heat demand	670 MWh	699 MWh
Measured heat demand	640 MWh	704 MWh

Table 6.1 Thermal characteristics of the building used to calculate the heat demand. Comparison with the measured heat demand.

The calculated annual heat demand is quite close to the measured one (within 5%). The heat load model permits a recalculation of the heat demand of a building on the basis of its physical thermal characteristics.

6.1.6 Comparison with the BKL-Method

The BKL-Method is a simple model used to determine the heating requirement of a building [4]. Passive solar gains are explicitly computed. The heat demand is calculated day by day. A "simple" house is defined as having only one window facing south-east. The heat losses through the ground are neglected (or are included in the total specific heat loss coefficient). Dimensions and thermal characteristics of the house are reported in table 6.2.

	Area or volume	U-value or air change rate	Specific heat loss
Facade S-E : window	(5 x 2) = 10 m^2	1.64 W/m^2K	16.4 W/K
: wall	(10 x 2.5 - 10) = 15 m^2	0.2 W/m^2K	3 W/K
Facade N-E : wall	(10 x 2.5) = 25 m^2	0.2 W/m^2K	5 W/K
Facade N-W : wall	(10 x 2.5) = 25 m^2	0.2 W/m^2K	5 W/K
Facade S-W : wall	(10 x 2.5) = 25 m^2	0.2 W/m^2K	5 W/K
Roof	(10 x 10) = 100 m^2	0.14 W/m^2K	14 W/K
Air change rate (assumed constant)	240 m^3	0.5 ach/h	39.6 W/K
Total			88 W/K

Table 6.2 Dimensions and thermal characteristics of the house.

The U-value of the window is very low, and corresponds to a double-glazed window with a selective surface. Nevertheless, the programme treats the window as a double glazed window, and the solar-transmittance is around 0.7. This is taken into account by the reduction factor for curtains and dirt. This latter is set to 0.5. A solar equivalent area for passive gains collection may be determined for the window. If the vertical south-east insolation is used, the solar equivalent area corresponds to the solar effective area. Related parameters are reported in table 6.3.

Window:	(5m x 2m)	10 m^2
Frame:	thickness	0.1 m
Reduction factor:	frame	0.864
	glazing	0.7
	curtains and dirt	0.5
	total	0.3
Solar effective area		3 m^2

Table 6.3 Dimensions and transmittance properties of the window.

Internal gains are set to 4.2 kWh/day; they reduce the set-point temperature by 2 K. The time constant of the house is fixed at 2 days. (If a layer of 10 cm of concrete contributes to the

effective heat capacity of the house, an area of about 100 m^2 provides half of the required value). The parameters used by the hour by hour model are reported in table 6.4.

Total specific heat losses:	88 W/K
Solar effective area:	3 m^2
Time constant:	2 days
Set-point temperature:	20 °C
Reduction due to internal gains:	2 K
No heating outdoor temperature:	12 °C
Maximum allowed indoor temperature:	25 °C

Table 6.4 Parameters used with the hour by hour model.

The weather data from Geneva, Switzerland is used (altitude: 400 m, latitude: 46.2° N, longitude: 6.1° E). The hourly measured values from July 1991 to June 1992 are processed to produce an adequate weather data file for the BKL programme. The heat demand is calculated with the two methods and a monthly comparison is made (see table 6.5).

Heat requirement kWh	BKL-Method	Hour by hour method	Difference
July	0	0	-
August	0	0	-
September	0	13	-
October	283	310	9%
November	673	676	0%
December	957	952	-1%
January	1'011	1'013	0%
February	654	669	2%
March	408	419	3%
April	138	244	77%
May	0	50	-
June	0	12	-
Total	4'124	4'357	6%

Table 6.5 Comparison of the heating requirement calculated with the two methods.

The comparison is quite satisfactory. The main difference is due to the amount of passive solar gains calculated: they are smaller with the hour by hour method. However, the BKL-Method assumes a high thermal inertia inside the house, so that daily passive gains are used during the whole day.

6.2 The "Passive" Problem

6.2.1 Definition of the Problem

One assume that a house, specifically designed to take advantage of passive solar gains, will require energy for heating only during the coldest months of the winter, when solar gains are practically negligible. This would mean that the load profile during the heating period of these houses may greatly differ from that of "conventional" houses (see Fig. 6.1).

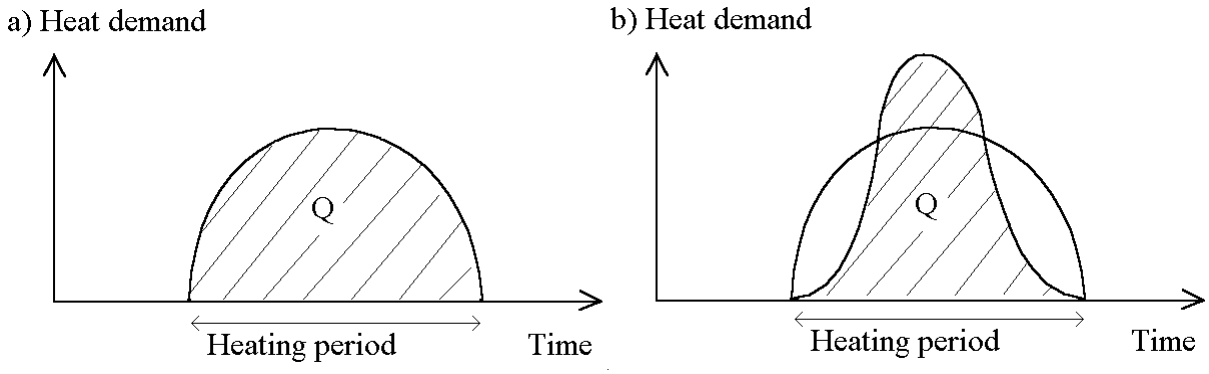

Fig. 6.1 a) Load profile of "conventional" houses. b) Load profile of "passive" houses. The number of houses is such that the annual heat demand Q is the same in both cases.

If such a difference may occur, the thermal performances of a CSHPSS (Central Solar Heating Plant with Seasonal Storage) will be penalised by "passive" housing, as the thermal energy is needed later in the winter, with larger heat rates and higher temperatures than those at the beginning and the end of the heating period.

It should be noted that the distinction between "conventional" and "passive" houses is not perfectly clear, as a "conventional" house still receives some passive solar gains. In our case, the distinction is made in the manner the passive solar gains are assessed. With a "passive" house, the passive solar gains are explicitly calculated (solar effective area), whereas in the case of "conventional" house, they are implicitly taken into account by using an outdoor temperature heat cut-out limit (as in the Degree-Day approach).

6.2.2 Formulation of the Problem

Three types of houses are defined:

A: a "conventional" house; its annual heat demand (for typical winter weather corresponding to the Swiss plateau) is assumed to be 500 MJ/m^{2}y or 140 kWh/m^{2}y (space heating (sh) and domestic hot water (dhw)).

B: a "passive" house; its annual heat demand is assumed to be 300 MJ/m^{2}y or 80 kWh/m^{2}h (sh + dhw). The passive solar gains are collected through windows facing south; (10 m^2 per 100 m^2 floor area).

C: an "extremely passive" house; its annual heat demand is assumed to be 300 MJ/m^{2}y or 80 kWh/m^{2}y(sh + dhw). Its total specific heat losses (per square meter of floor area), are assumed to be the same as the "conventional" house. The reduction of the heat demand, from 500 to 300 MJ/m^{2}y, is achieved by passive solar gains only.

The domestic hot water requirement (per square meter of floor area), is assumed to be the same for every type of house.

Three annual loads of 1'000 MWh (sh + dhw) are formed by a set of each type of houses. The annual load profile is then calculated for the three situations and then compared on a daily basis.

It should be noted that the annual heat demand is quite low, even with conventional houses. In consequence these latter have to be carefully designed, relatively well insulated and air tight.

6.2.3 Heat Load Parameters

The domestic hot water requirement is set to 125 MJ/m^{2}y or 35 kWh/m^{2}y, according to measurements of an existing housing area [5]. Assuming that a house unit has an area of 100 m^2, a set of "conventional" and "passive" houses are formed to produce a total annual heat load of 1'000 MWh (cf. table 6.6).

	"Conventional" house	"Passive" house
Annual heat demand	140 kWh/m^{2}y (100%)	80 kWh/m^{2}y (100%)
Domestic hot water (dhw)	35 kWh/m^{2}y (25%)	35 kWh/m^{2}y (44%)
Space heating (sh)	105 kWh/m^{2}y (75%)	45 kWh/m^{2}y (56%)
Total load	1'000 MWh/y	1'000 MWh/y
Total dhw	250 MWh/y	440 MWh/y
Total sh	750 MWh/y	560 MWh/y
Number of house units	70	120

Table 6.6 Set of "conventional" and "passive" houses to form a total annual heat load of 1'000 MWh.

The simple model described in the first section of the chapter is used to calculate the space heating requirement. Weather data measured in Geneva (Switzerland) during one year (from July 1991 to June 1992) is used.(Altitude: 400 m, latitude: 46.2° N, longitude: 6.1° E). The yearly mean outdoor temperature was 11.8 °C that year, with extreme daily values of -5 °C and +28 °C. The Degree-Days 12/20 were measured at 2'900 Kday and the global horizontal radiation at 1'260 kWh/m^{2}year. (Degree-Days 12/20 means that the degree-days are established in relation to an indoor temperature of 20 °C and taken into account only when the daily outdoor temperature is below 12 °C.)

With "conventional" houses, all the parameters of the heat load model are fixed except the total specific heat loss coefficient. This latter is adjusted so that the calculated heat requirement matches the prescribed one.

The solar effective area is assumed to be 30% of the window area. With the set of "passive" houses, it corresponds to 375 m^2. The annual heating requirement is adjusted with the total specific heat loss coefficient. The value of this latter, reported per house, will affect the time constant of the housing and the correction to the indoor temperature due to internal gains. If the heat loss coefficient per house is roughly two times smaller, the time constant and the temperature correction will be two times larger.

In the case of "extremely passive" houses, the solar effective area is adjusted to satisfy the prescribed heating requirement. The load parameters, corresponding to each set of houses, are listed in table 6.7.

Set of houses	"Conventional"	"Passive"	"Extremely passive"
Total specific heat losses	11 kW/K (150 W/K per house)	11 kW/K (90 W/K per house)	18.3 kW/K (150 W/K per house)
Solar effective area	0 m^2	375 m^2	2'300 m^2
Time constant	1 day	2 days	4 days
Indoor set-point temperature	20 °C	20 °C	20 °C
Correction due to internal gains	-1 K	-2 K	-1 K
Outdoor temperature limit to cut the heating	12 °C	12 °C	12 °C
Maximum indoor temperature	25 °C	25 °C	25 °C
Calculated space heating requirement	725 MWh/y	545 MWh/y	550 MWh/y

Table 6.7 Heat load parameters corresponding to each set of houses.

The outdoor temperature heat cut-out limit has no influence with the set of "passive" and "extremely passive" houses. The case with "extremely passive" houses led to an unrealistic situation, with about 20 m^2 of solar effective area per house, or some 60 m^2 of windows facing south! The effective heat capacity of the house also had to be increased by a factor of 4 in order to store the collected passive gains.

This example shows that a low annual heating requirement can not be achieved by passive solar gains only, but requires a careful design of the house in order to decrease the heat losses. This conclusion is valid for the type of climate taken in consideration here. This is particularly true for northern European climates.

6.2.4 Load Profiles

The daily space heating load profile is only shown for the sets of "conventional" and "passive" houses (cf. Fig. 6.2). (The case with "extremely passive" houses is not realistic). The "passive" heating load is always smaller than the "conventional" one. (The annual space heating requirement is smaller than the "conventional" one: 545 MWh rather than 725 MWh). The total specific heat loss coefficient is the same in both cases. The difference in the heating requirement is due to internal gains that are larger with the set of "passive" houses (more houses) and the passive solar gains that are also larger with "passive" houses.

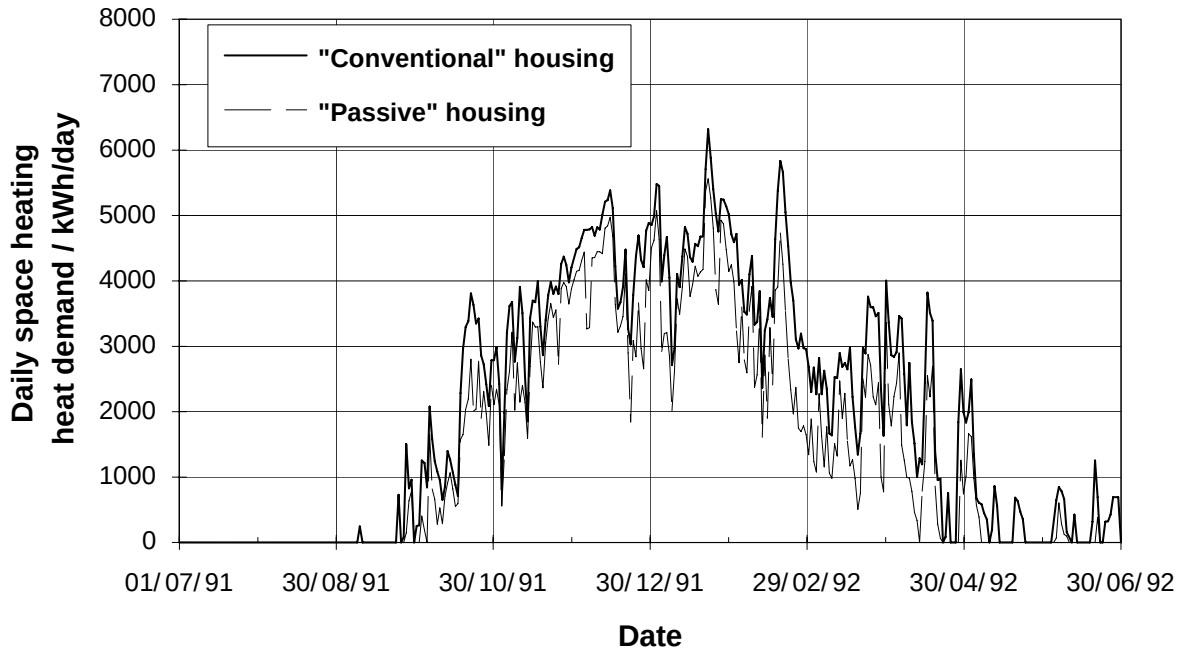

Fig. 6.2 Daily space heating heat demand for the sets of "conventional" and "passive" houses.

The domestic hot water requirement is assumed to be constant over the year. The total heat demand is shown in Fig. 6.3 for the two cases with daily values.

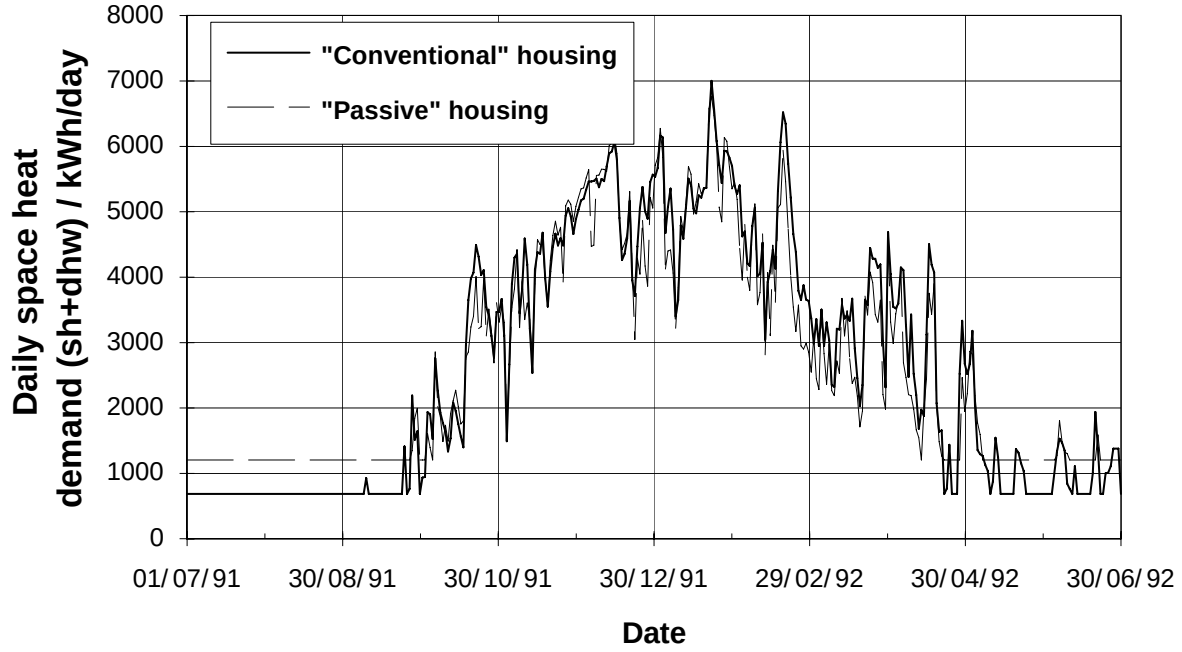

Fig. 6.3 Daily heat demand (space heating + domestic hot water) for the sets of "conventional" and "passive" houses.

The shape of the load profile is quite similar for these two cases. The load profile hypothesis (cf. Fig. 6.1) is not verified. The maximum daily heat demand is nearly equal in both cases. With the set of "passive" houses, the summer heat demand is larger, which favorises the need for short term storage.

6.2.5 Load Model without Solar Effective Area

The number of parameters is reduced from 7 to 4 if the solar gains are not explicitly calculated; the south vertical insolation is also not required for the calculation.

The heat demand for the set of "passive" houses is recalculated without a solar effective area. In order to obtain the same annual heat demand (550 MWh/y), the correction to the indoor set-point temperature is increased to include the passive solar gains with the internal gains. This is realised with a corrected indoor set-point temperature of 15.5 °C rather than 18 °C. The three other load parameters are not changed (H, Tin and Tnh). A comparison of the monthly heat demand (calculated with and without a solar effective area) is shown in Fig. 6.4.

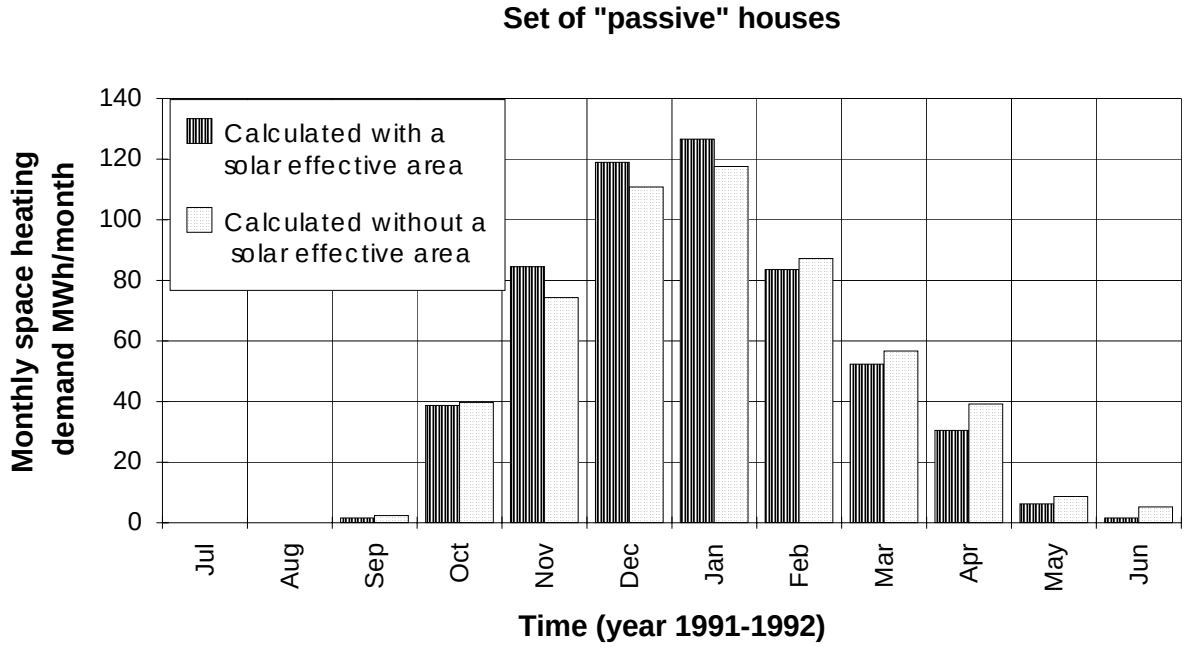

Fig. 6.4 Monthly heat demand calculated with and without a solar effective area for the set of "passive" houses.

The difference between the monthly values remains below 10% for the coldest months when considering the total heat demand (sh + dhw). The peak power loads, assuming they occur with a temperature difference of 20 K (indoor - outdoor), are also reduced by approximately 10%.

The outdoor temperature heat cut-out limit represents a valuable criterion for determining the length of the heating period. For the case in question it lasted from mid-September to mid-June. In order to assess the importance of the internal and passive solar gains, the total heat demand is calculated during the heating period for an indoor temperature of 20, 18 and 15.5 °C respectively, without using the outdoor temperature heat cut-out limit. The annual heat demand corresponds to the total heat losses of the houses during the heating period when it is calculated with the actual indoor temperature of 20 °C.

The heat losses of the "passive" house are reduced by 16% with internal gains and 18% with passive solar gains. Similar values are obtained (13% and 17% respectively) if the outdoor temperature heat cut-out limit is used.

6.3 Conclusion

According to the definitions given in section 6.2.2, a set of "passive" houses presents a load profile during the heating period which is similar to a set of "conventional" houses. The passive problem, as defined in section 6.2.1, will not occur if the passive solar gains of a low energy house do not exceed 20% of its heat losses during the heating period. The main differences with "conventional" housing are:

- the proportion of domestic hot water, which is more important with low energy buildings;
- the temperature level of the heat distribution, which should be lower with low energy houses;
- the density of the consumer which is lower with low energy buildings; (if they are single family houses, the distribution network is larger).

Unlike the last difference, the first two are beneficial to the thermal performances of a central solar plant.

The space-heating heat demand may be calculated using a 7 parameter model, so that the passive solar gains are explicitly computed. They may be implicitly accounted for and the model is reduced to 4 parameters, requiring only the outdoor temperature for the meteorological variable. If the passive solar gains reduce the total heat losses of a building by 20% or less, then the difference between the two methods is not as important; (of the same order of magnitude as the accuracy of the model). In that case, the short version of the load model (4 parameters) is prefered.

7. HEAT LOAD MODEL FOR A "CSHPSS"

7.1 Characteristics of the Heat Load Model

The model has to be simple, flexible and should be sufficiently realistic so as to be able to reproduce the main features of an actual load. The design of the system should not be sensitive to the differences between the calculated and the actual heat demand. In particular, the model should:

- give the same annual energy consumption;
- present similar peak power loads;
- determine the correct temperature levels of the heat to be distributed;
- and reproduce as closely as possible the monthly energy requirements of the consumer.

The following variables have to be calculated:

- the forward temperature of the heat carrier fluid to the consumer;
- the return temperature of the heat carrier fluid from the consumer;
- and the total flow rate in the distribution network.

7.2 Procedure to Calculate the Load Variables

We assume that one distribution network is used for domestic hot water and space heating requirements ("two pipe" distribution network). The heat demand is calculated on an hourly basis. It is assessed by the sum of three parts:

- Psh : the space-heating heat demand [kJ/h];
- Pdhw : the domestic hot water requirement [kJ/h];
- Ploss : the heat losses of the distribution network [kJ/h].

Heat capacitive effects in the distribution network are not considered. The forward and return temperatures of the network are calculated according to the outdoor temperature, then the flow rate is entirely determined.

7.3 Space-heating Heat Demand

The space-heating heat demand may be calculated using the load model described in the previous chapter. According to the accuracy of the model, the use of a solar effective area is not necessarily required for the computation of the passive solar gains (see chapter 6). The number of parameters is reduced from 7 to 4:

H: total specific heat losses of the housing; (transmission and ventilation losses) [kJ/hK];
Tin: indoor set-point temperature [°C];
Tnh: outdoor temperature heat cut-out limit [°C];
ΔTingains: correction to the indoor set-point temperature due to the internal and passive solar gains [K].

The hourly space-heating heat demand is calculated using the following relation:

$$\text{If } T_{out} < T_{nh} \text{ Then } P_{sh} = H \cdot [T_{in} - \Delta T_{ingains} - T_{out}] \quad (7.1a)$$

$$\text{Else } P_{sh} = 0 \quad (7.1b)$$

Tout: the outdoor temperature of the air [°C].

The outdoor temperature heat cut-out limit has to be lower than the indoor set-point temperature corrected by the effect of internal and passive solar gains. A default value is to set it 8 K below the indoor set-point temperature.

If the correction to the indoor set-point temperature is set to 0, then the model is compatible with the Degree-Day approach. The annual space-heating requirement, calculated using an hourly rather than a daily outdoor temperature heat cut-out limit (Tnh), does not differ by more than a few percent (with the Swiss weather data used in chapter 6).

7.4 Domestic Hot Water Requirement

A daily profile is given on an hourly basis. It should be representative of typical domestic hot water use. Seasonal variations are accounted for by a correction factor given on a monthly basis. These values have to be given according to the consumer under consideration. Some knowledge and experience is thus required.

7.5 Distribution Network Losses

The losses of the distribution network depend mainly on the mean temperature of the heat carrier fluid and the mean outdoor temperature of the air. Other factors such as rain, snow, etc. may have some influence. If the pipes are well insulated, seasonal variations are probably not significant. An average constant value, representing the outdoor temperature of the air, can be used throughout the year.

7.6 Forward and return temperature

The forward temperature of the fluid in a distribution network is usually controlled and set to a desired value which depends on the outdoor temperature.

The return temperature is difficult to assess, as the heat requirement of the housing, the characteristics of the distribution network and the thermal performances of the heat devices in the housing are involved. One assumes that the return temperature may be described in the same way as the forward temperature, with a similar relation. An example is given in Fig. 7.1.

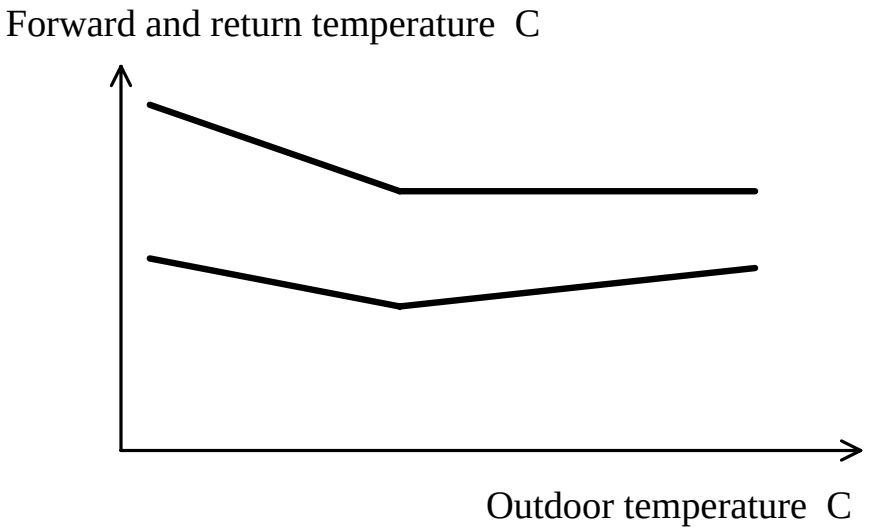

Fig. 7.1 Dependence example of the forward and return temperatures of a distribution network on the outdoor temperature.

The thermal performances of the solar plant are also sensitive to the temperature level of the return temperature. When a solar plant is designed and optimised, one has to ensure that the return temperature will be as low as possible, requiring that the distribution network and the housing be carefully designed for this purpose.

8. CONCLUSION

Typical CSHPSS-systems with a seasonal duct store in the ground, designed to be operated at medium or high temperature, have been studied. Two basic system designs have been defined (with or without short-term buffer tank), based on the work achieved in Task VII of the International Energy Agency (Central Solar Heating Plants with Seasonal Storage).

Detailed programmes were used to assessed particular effects related to the simulation of such systems:

- A case study was performed to assess the influence of the weather data time-step on the simulated thermal performances. It can be concluded that the common use of hourly rather than finer meteorological data values, does not generate significant differences (< 2%) in the simulated collected energy.
- The heat capacitive effects of the collector array were assessed for specific examples. They showed that the resulting decrease of the mean collector efficiency may be significant for large heat capacity values in the collector array (> 10 kJ/m^{2}K).
- The heat capacitive effects of the ground heat exchanger can enhance the mean collector efficiency. These effects are negligible, provided that a sufficiently large buffer tank (> 60 litres/m^2 of collector area) and/or a performant collector array are used.
- The local solutions in the duct store were computed in great detail. Accurate simulations and proper sensitivity analysis require a flow- and temperature-dependent fluid-to-ground thermal resistance. The axial effects, due to a varying temperature along the fluid channels in the boreholes, can be significant for deep boreholes (> 100 m) and low flow rates (< 0.5 m^3/hour per borehole). They can be taken into account with the concept of effective fluid-to-ground thermal resistance. Finally, the local solutions should be able to take into consideration a connection in series of the boreholes, as well as a vertical division of the store volume.

The detailed programmes served as a basis to develop TRNSYS simulation tools, and to identify the necessary improvements to be made in the duct store component. The advantage in using the TRNSYS simulation programme is that it is known world-wide. The set-up of TRNSYS systems was verified with the detailed programmes. Some practical problems related to the TRNSYS systems were discussed. TRNSYS simulation made over a long period (20 years) provided examples of the heat capacitive effects of the collector array on the collected energy. The system design with a short-term buffer tank seems to be promising, as some preliminary simulations showed a significant improvement of the system performances and lower extreme temperatures in the collector array (solar heat increased by 10% and maximum fluid temperature decreased by 10 K). Furthermore, this type of system allows each subsystem to be operated independently using its optimum characteristics. Finally, a list of modifications is given so that the simulation tools can be used to optimised future systems.

A simple load model is presented, which can simulate the total space heating demand of a group of houses. The problem of passive solar gains is addressed. Using typical weather data of the Swiss plateau, the passive solar gains will not penalise the thermal performances of a CSHPSS-system if they do not exceed 20% of the heat losses of the houses during the heating period. Lastly, a procedure to calculate the load variables of a CSHPSS-system is proposed.

REFERENCES

Chapter 3:

1. J.-O. Dalenbäck, Solar Heating with Seasonal Storage, Some Aspects of the Design and Evaluation of Systems with Water Storage, Document D21:1993, Department of Building Service Engineering, Chalmers University of Technology, Göteborg, Sweden (1993).

2. G. Hellström, Ground Heat Storage - Thermal Analyses of Duct Storage Systems. Theory, Thesis, Department of Mathematical Physics, University of Lund, Sweden (1991).

3. D. Pahud, Etude du Centre Industriel et Artisanal Marcinhès à Meyrin (GE). Rapport Final, Groupe de Physique Appliquée et Centre Universitaire pour l'Etude des Problèmes de l'Energie, Université de Genève, Switzerland (septembre 1993).

4. D. Pahud, Analyse énergétique de l'immeuble industriel "Marcinhès" à Meyrin (GE), Thèse n° 2645, Groupe de Physique Appliquée, Université de Genève, Switzerland (1993).

5. G. Hellström, Duct Ground Heat Storage Model, Manual for Computer Code, Department of Mathematical Physics, University of Lund, Sweden (1989).

6. L. Mazzarella, Duct Thermal Storage Model. Lund - DST. TRNSYS Version 1990, ITW, Universität Stuttgart, Germany, Dipartimento di Energetica, Politechnico di Milano, Italy (1990).

7. TRNSYS - A Transient Simulation Program. Version 13.1, Solar Energy Laboratory, University of Wisconsin, Madison (1990).

8. Hellström G., Mazzarella L. and Pahud D. (1996) Duct Ground Heat Storage Model. Lund - DST. TRNSYS 13.1 Version January 1996. Department of Mathematical Physics, University of Lund, Sweden.

9. J.-O. Dalenbäck, Central Solar Heating Plants with Seasonal Storage, Status Report, Document D14:1990, Swedish Council for Building Research, Stockholm, (Final report IEA SH&CP, Task VII) (1990).

10. L. Mazzarella, The MINSUN Program. Application and User's Guide, Dipartemento di Energetica, Politechnico di Milano, Italy (1989).

11. L. Mazzarella, MINSUN 6.0 - NEWMIN 2.0. A Revised IEA Computer Program for Performance Simulation of Energy Systems with Seasonal Thermal Energy Storage, Proceedings Thermastock' 91, 5th International Conference on Thermal Energy Storage, Paper No. 3.5-1, Scheveningen, The Netherlands (1991).

12. J. A. Duffie and W. A. Beckmann, Solar Engineering of Thermal Processes, Second edition, John Wiley & Sons, Inc., USA (1991).

13. D. S. Breger, Final Engineering and Design Analysis of the Central Solar Heating Plant with Seasonal Storage at the University of Massachusetts / Amherst, Final Report, Department of Mechanical Engineering, University of Massachusetts at Amherst, USA (July 1994).

14. H. Seiwald and E. Hahne, Sensitivity Analysis of a Central Solar Heating System with High Temperature Duct Seasonal Storage, Proceedings Calorstock' 94. 6th International Conference on Thermal Energy Storage, pp 705-712, Espoo, Finland (August 1994).

15. B. Eftring and G. Hellström, Stratified Storage Temperature Model - Manual for Computer Code, Department of Mathematical Physics, University of Lund, Sweden (1989).

16. P. Isaksson and L. O. Eriksson, Matched Flow Solar Collector Model for TRNSYS 13.1-Users Manual, Version MFC 1.0β, August 1993, Royal Institute of Technology, Stockholm, Sweden (1993).

Chapter 4:

1. L. Mazzarella, The MINSUN Program. Application and User's Guide, Dipartemento di Energetica, Politechnico di Milano, Italy (1989).

2. TRNSYS - A Transient Simulation Program. Version 13.1, Solar Energy Laboratory, University of Wisconsin, Madison (1990).

3. B. Eftring and G. Hellström, Stratified Storage Temperature Model - Manual for Computer Code, Department of Mathematical Physics, University of Lund, Sweden (1989).

4. G. Hellström, Duct Ground Heat Storage Model, Manual for Computer Code, Department of Mathematical Physics, University of Lund, Sweden (1989).

5. G. Hellström and J. Bennet, Model of Aquifer Storage System, Doublet Well, Manual for Computer Code, Department of Mathematical Physics, University of Lund, Sweden (1989).

6. L. Mazzarella, Stratified Storage Temperature Model. Lund - SST. TRNSYS Version July 1990, ITW, Universität Stuttgart, Germany, Dipartimento di Energetica, Politechnico di Milano, Italy (1990).

7. L. Mazzarella, Multi-flow Stratified Thermal Storage Model with Layers with Memory. PdM - MST. TRNSYS Version September 1992, ITW, Universität Stuttgart, Germany, Dipartimento di Energetica, Politechnico di Milano, Italy (1992).

8. L. Mazzarella, Multi-flow Stratified Thermal Storage Model with Full Mixed Layers. PdM - XST. TRNSYS Version September 1992, ITW, Universität Stuttgart, Germany, Dipartimento di Energetica, Politechnico di Milano, Italy (1992).

9. L. Mazzarella, Duct Thermal Storage Model. Lund - DST. TRNSYS 13.1 Version March 1993, ITW, Universität Stuttgart, Germany, Dipartimento di Energetica, Politechnico di Milano, Italy (1993).

10. D. S. Breger, Final Engineering and Design Analysis of the Central Solar Heating Plant with Seasonal Storage at the University of Massachusetts / Amherst, Final Report, Department of Mechanical Engineering, University of Massachusetts at Amherst, USA (July 1994).

11. H. Seiwald and E. Hahne, Sensitivity Analysis of a Central Solar Heating System with High Temperature Duct Seasonal Storage, Proceedings Calorstock' 94. 6th International Conference on Thermal Energy Storage, pp 705-712, Espoo, Finland (August 1994).

12. M. Lehmet, Competitive Seasonal Solar Systems for Swedish Conditions - Preliminary Results of a Parameter Study, Proceedings 1994 Workshop on Large-scale Solar Heating, pp 145-147, Gothenburg, Sweden (August 1994).

13. O. Olesen, Manual for SAESONSOL version 3.0, Medelelse No 254, Technical University of Denmark (1993).

14. K. Duer, Parameter Study of a Solar Heating Plant with 100'000m3 Duct Storage, Proceedings 1994 Workshop on Large-scale Solar Heating, pp 139-144, Gothenburg, Sweden (August 1994).

15. P. Isaksson and L. O. Eriksson, Matched Flow Solar Collector Model for TRNSYS 13.1-Users Manual, Version MFC 1.0β, August 1993, Royal Institute of Technology, Stockholm, Sweden (1993).

16. G. Hellström, Thermal Response Test at Bedrock Heat Store in Luleå, Department of Mathematical Physics, Lund Institute of Technology, Sweden (1989).

17. G. Hellström, Ground Heat Storage - Thermal Analyses of Duct Storage Systems. Theory, Thesis, Department of Mathematical Physics, Lund University, Sweden (1991).

Chapter 5:

1. TRNSYS - A Transient Simulation Program. Version 13.1, Solar Energy Laboratory, University of Wisconsin, Madison (1990).

2. L. Mazzarella, Duct Thermal Storage Model. Lund - DST. TRNSYS Version 1990, ITW, Universität Stuttgart, Germany, Dipartimento di Energetica, Politechnico di Milano, Italy (1990).

3. G. Hellström, Duct Ground Heat Storage Model, Manual for Computer Code, Department of Mathematical Physics, University of Lund, Sweden (1989).

4. L. Mazzarella, Multi-flow Stratified Thermal Storage Model with Full Mixed Layers. PdM - XST. TRNSYS Version September 1992, ITW, Universität Stuttgart, Germany, Dipartimento di Energetica, Politechnico di Milano, Italy (1992).

5. B. Eftring and G. Hellström, Stratified Storage Temperature Model - Manual for Computer Code, Department of Mathematical Physics, University of Lund, Sweden (1989).

6. P. Isaksson and L. O. Eriksson, Matched Flow Solar Collector Model for TRNSYS 13.1-Users Manual, Version MFC 1.0β, August 1993, Royal Institute of Technology, Stockholm, Sweden (1993).

7. PRESIM - A Preprocessor for Producing TRNSYS Input Data. Version 2.0, SERC, University College of Falung/Borlänge, Sweden (1991).

8. R. Perez, R. Stewart, R. Seals, T. Guertin, The Development and Verification of The Perez Diffuse Radiation Model, Report SAND88-7030, Sandia National Laboratories, Albuquerque, New Mexico, USA (1988).

9. J. Claesson, Thermodynamics of Sensible Heat Storage Systems. Thermality Concept, Department of Mathematical Physics, Lund, Sweden (August 1979).

10. J.-O. Dalenbäck, Solar Heating with Seasonal Storage, Some Aspects of the Design and Evaluation of Systems with Water Storage, Document D21:1993, Department of Building Service Engineering, Chalmers University of Technology, Göteborg, Sweden (1993).

Chapter 6:

1. C.-A. Roulet, Energétique du Bâtiment I, Presses plolytechniques romandes, Lausanne, Switzerland (1987).

2. European Standard, Thermal Performance of Buildings, Calculation of Energy Use for Heating, Residential Buildings. European Committtee for Standardization, Brussels, Belgium (1992).

3. D. Pahud, Etude du Centre Industriel et Artisanal Marcinhès à Meyrin (GE). Rapport Final, Groupe de Physique Appliquée et Centre Universitaire pour l'Etude des Problèmes de l'Energie, Université de Genève, Switzerland (septembre 1993).

4. K. Källblad, The BKL-Method Computer Programme, User Manual, Report TABK--94/3019, Department of Building Science, Lund University, Lund, Sweden (1994).

5. J.-O. Dalenbäck, Solar Heating with Seasonal Storage, Some Aspects of the Design and Evaluation of Systems with Water Storage, Document D21:1993, Department of Building Service Engineering, Chalmers University of Technology, Göteborg, Sweden (1993).